drugs and drug candidates

MDPI

Review

Therapeutic Perspectives of Metal Nanoformulations

Tawhida Islam [1], Md. Mizanur Rahaman [1], Md. Nayem Mia [1], Iffat Ara [1], Md. Tariqul Islam [1], Thoufiqul Alam Riaz [2,3], Ana C. J. Araújo [4], João Marcos Ferreira de Lima Silva [5], Bruna Caroline Gonçalves Vasconcelos de Lacerda [6], Edlane Martins de Andrade [6], Muhammad Ali Khan [1], Henrique D. M. Coutinho [4,*], Zakir Husain [1] and Muhammad Torequl Islam [1,*]

1 Department of Pharmacy, Bangabandhu Sheikh Mujibur Rahman Science and Technology University, Gopalganj 8100, Bangladesh
2 School of Medicine, Department of Medical Science, Jeonbuk National University, Jeonju 561-756, Republic of Korea
3 Nutrition and Immunology, Technical University Munich, 81675 Munich, Germany
4 Department of Biological Chemistry, Regional University of Cariri-URCA, Crato 63100-000, CE, Brazil
5 Department of Physical Education, Centro Universitário Doutor Leão Sampaio, Juazeiro do Norte 63024-015, CE, Brazil
6 CECAPE College, Av. Padre Cícero, 3917-São José, Juazeiro do Norte 63024-015, CE, Brazil
* Correspondence: hdmcoutinho@gmail.com (H.D.M.C.); dmt.islam@bsmrstu.edu.bd (M.T.I.)

Abstract: In recent decades, acceptance of nanoparticles (NPs) in therapeutic applications has increased because of their outstanding physicochemical features. By overcoming the drawbacks of conventional therapy, the utilization of metal NPs, metal-oxide, or metal supported nanomaterials have shown to have significant therapeutic applications in medicine. This is proved by a lot of clinical and laboratory investigations that show improved treatment outcomes, site-specific drug delivery, and fewer side effects compared to traditional medicine. The metal NPs interaction with living cells (animal and plant) showed many ways to develop therapeutic models with the NPs. Despite all of the advancements that science has achieved, there is still a need to find out their performance for long-term use to solve modern challenges. In this regard, the present documentation reviews some potential metals, including silver (Ag), gold (Au), zinc (Zn), copper (Cu), iron (Fe), and nickel (Ni) NPs, as therapeutic agents in various areas such as anticancer, antimicrobial, antidiabetic, and applicable for the treatment of many other diseases. Depending on the outstanding ongoing research and practical trials, metal-based NPs can be considered the hope of prospective modern therapeutic areas.

Keywords: metal nanoparticles; nanotherapy; therapeutic uses; targeted strategy

Citation: Islam, T.; Rahaman, M.M.; Mia, M.N.; Ara, I.; Islam, M.T.; Alam Riaz, T.; Araújo, A.C.J.; de Lima Silva, J.M.F.; de Lacerda, B.C.G.V.; de Andrade, E.M.; et al. Therapeutic Perspectives of Metal Nanoformulations. *Drugs Drug Candidates* **2023**, *2*, 232–278. https://doi.org/10.3390/ddc2020014

Academic Editors: Tanja Soldatović and Snežana Jovanović-Stević

Received: 23 December 2022
Revised: 10 February 2023
Accepted: 6 March 2023
Published: 13 April 2023

1. Introduction

The implementation of nanoparticles (NPs) for the treatment and diagnosis of disease is a revolutionary concept that has been developed over the past few decades. The nanotechnological approach can be divided into two branches: one is nanodevices and the other is nanomaterials. The nanodevice can be defined as such tiny devices at the nanoscale range, which includes microarrays and some devices such as respirocytes [1–3].

Particles smaller than 100 nanometers (nm) in any one of the dimensions are considered nanomaterials. Biomedical science found successful result by using nanoparticles as therapeutic agents in the treatment of various diseases. As it is selective on the target organ and receptors, it overcomes several limitations of conventional therapy, such as nonspecificity, unwanted side effects, less efficiency, and low bioavailability [4].

Therefore, current research projects are considerably more focused on developing and designing new drug delivery systems, and the most promising area is ensured by NPs for their uniqueness in biological and physicochemical characteristics, as they can deliver molecules to specific locations in the body [5].

The therapeutic molecules which are insoluble in water can be complexed with NPs, resulting in greater bioavailability and significantly fewer physiological barriers; for example, NP carriers assist medication in passing the blood–brain barrier (BBB) [6–8]. Nevertheless, because it is targeted, it will require lower doses than conventional therapy, and the therapeutic index will be higher as it will minimize the toxicity in the biological system. The utilization of NPs in various fields of the health sector is possible because of their ability to provide a visual image of the targeted delivery location by using some agents; moreover, their pathway can be tracked.

Several studies have recently focused on the method of producing metal NPs using green synthesis, which has shown positive results against pathogens, cancer cells, helminths, fungi, etc. using the metal NPs Zn, Ag, Au, Pt, Mn, Ni, and Ti [9]. Currently, among other NPs, Ag-NPs are one of the top listed compounds being researched [10]. In 1857, Michael Faraday was the first person to study Au-NPs in a colloidal system and report Au-NP's optical features [11].

This documentation reviewed physicochemical properties of the NPs Au, Ag, Cu, Fe, Ni, and Zn and generated a review of the recent year's progression for their use as nanomedicine with their application as targeted delivery in numerous physical disorders.

1.1. Significance of Metals in Human Body

For diagnostic and treatment purposes, metals are used in organic systems as medicine [12]. There are some metals, such as mercury (Hg), cadmium (Cd), and arsenic (As), that are considered toxic when they cross a certain limit, but some metals are necessary for the body's enzymatic and metabolic functions. For instance, there are metalloproteins which contain metal ions as co-factors, and a greater portion of proteins are in this category. There is a minimum 1000–3000 human proteins which contain a Zn ion as a co-factor [13]. The comparative presence of metals in the human body shown in Table 1.

Table 1. Concentration of metals in some human organs [14].

Metals	Liver (ppm)	Kidney (ppm)	Lung (ppm)	Heart (ppm)	Brain (ppm)	Muscle (ppm)
Iron	16,769	7168	24,967	5530	4100	3500
Manganese	138	79	29	27	22	<4–40
Nickel	<5	<5–12	<5	<5	<5	<15
Zinc	5543	5018	1470	2772	915	4688
Cobalt	<2–13	<2	<2–8	-	<2	150
Copper	882	379	220	350	401	85–305

1.2. Major Function of Metals in Human Body

Sections 1.2.1–1.2.7 aim to describe the significance of the selected metals in the general physiological functions of the human body.

1.2.1. Manganese (Mn)

Manganese is significant for development, metabolism, and the antioxidant system. Importantly, Mn is needed for amino acid, cholesterol, and carbohydrate metabolism and in bone and thyroxin formation.

Mn is required for the action of enzyme families, such as oxidoreductases, hydrolases, transferases, lyases, isomerases, and ligases. For normal immune protection, blood sugar control, creating cellular energy, and reproduction, Mn works with various organ systems. It is estimated by the National Research Council that for adults, 2 to 5 mg of dietary manganese per day is safe [15].

It is particularly important for the detoxification of superoxide free radicals, and it activates some metalloproteases. It assists the body in using biotin, thiamin, vitamin C, and choline. However, excessive intake can lead to a stage called manganism, which causes neuronal death and a Parkinson's-like syndrome [16].

1.2.2. Iron (Fe)

Fe is a vital component of hemoglobin (RBC) [17]. Fe aids in the metabolism of muscle and active connective tissue. It is needed for the synthesis of some hormones, neurological development, maintaining physical growth, and cellular functioning [18,19].

For the synthesis of DNA and electron transportation, Fe is important [20]. Fe deficiency is the reason for about 50% of the cases of anemia around the world, according to a WHO report [21].

1.2.3. Cobalt (Co)

Co is a part of cobalamin, or vitamin B12, and therefore, it is significant for the function of cells. Co is needed for the production of RBC and the production of antimicrobial compounds (antibacterial and antiviral). Cobalt plays a vital role in amino acid and protein generation and the formation of neurotransmitters. Co salt is used in the treatment of anemia [22].

1.2.4. Nickel (Ni)

For regulating the proper function of the human body, Ni is an essential micronutrient. This metal amplifies hormonal function and is also required in lipid metabolism [23]. Although the mechanism of toxicity is unknown, prolonged contact or higher intake can result in a variety of side effects, including cancer [24]. Ni is required in trace amounts for growth and reproduction [25]. It activates arginase and urease enzymes [12] and also inhibits some enzymes, for instance, acid phosphatase [26].

1.2.5. Copper (Cu)

Cu is highly involved in energy production, iron metabolism, the formation of connective tissue, and the activation of neuropeptides and neurotransmitters [17,18]. Ceruloplasmin (CP), a Cu-abundant enzyme involved in Fe metabolism, is mostly composed of Cu and accounts for approximately 95% of total Cu in human plasma [27]. Cu is also involved in various physiologic processes, including angiogenesis, brain development, pigmentation, neurohormone homeostasis, gene expression regulation, and immune system functioning [24], as well as providing protection against oxidative damage [28,29].

1.2.6. Zinc (Zn)

Zn is required in a variety of ways for cellular metabolism. Zn is mandatory for the activation of about 100 enzymes [30,31], and it has roles in the immune system, protein synthesis [32,33], wound healing [34], DNA synthesis, and cell division [35,36]. It assists the normal development of the fetus during pregnancy and is needed for further growth from the stage of childhood to adolescence [37,38]. Moreover, Prasad et al. demonstrated that Zn is responsible for a proper sense of smell and taste [39,40]. Because the human body cannot store zinc, it must be consumed on a regular basis to keep these functions running smoothly [41].

1.2.7. Gold (Au)

The average human body (for an average adult human weighing 70 kg) might contain about 0.2 mg of Au [42]. Significant health functions include helping to maintain our joints as well as facilitating the transmission of electrical signals throughout the body. It is necessary for the maintenance and function of the joints. Additionally, Au it is an excellent conductor of electricity, aiding in the transmission of electrical signals throughout the body [39]. Several cell-mediated immune responses to various mitogens and antigens are inhibited by gold compounds. This inhibition is accelerated by the Au's impact on macrophages [43].

1.3. Size, Shape, Material, and Surface of Nanoparticles

NPs range from 1 to 100 nm (Figure 1) and could be a sphere, cube, rod, plate, or star shape.

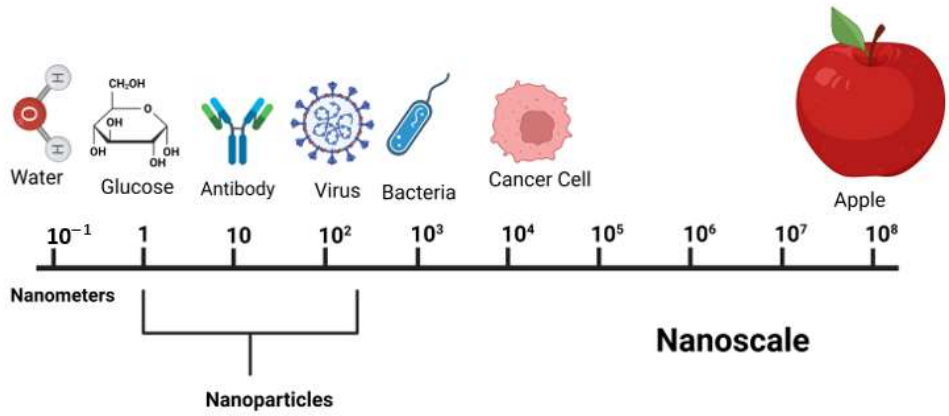

Figure 1. Sizes of nanoscale items in comparison to other relevant objects.

The surface of the NPs can be PEGylation or another coating, which might have present linkers containing surface functional group, surface charge, and targeting ligand (antibody, peptide, aptamer, etc.); see Figure 2. Nanomaterial size, shape, and surface coating are essential parameters that influence cell uptake and/or the pace and site-specific drug delivery from the system. The shapes of nanoparticles also play a crucial role in infrared absorption, which is particularly essential in phototherapy [44]. Rods are the most absorbent, followed by spheres, cylinders, and cubes [45].

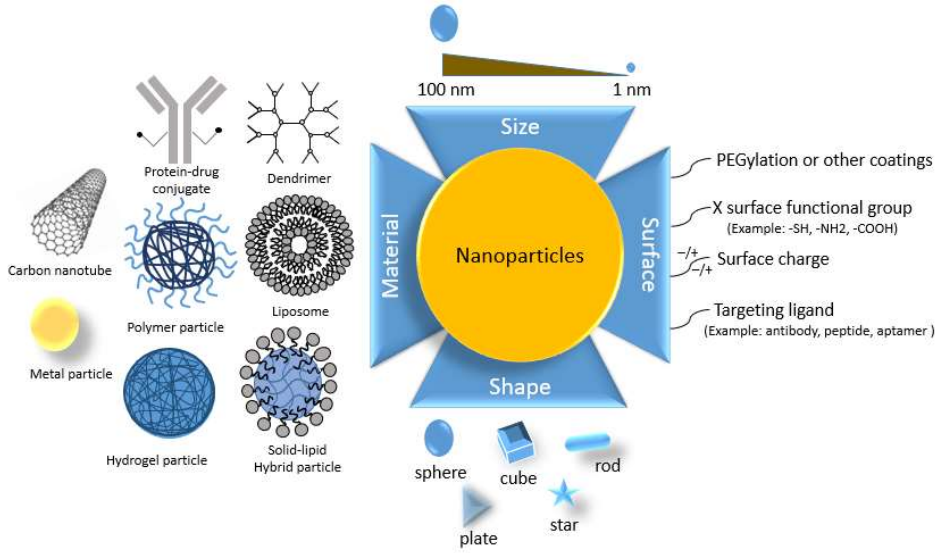

Figure 2. Size, shape, and surface material of nanoparticles.

1.4. Major Nanodrug Delivery Systems

This section will familiarize you with the various types of nanomedicine and provide a general idea for further research. Based on the recent approaches, polymeric, metallic, and ceramic NP drug delivery vehicles are widely used [8], such as liposomes [46], micelles [47], dendrimers [48], etc. A large number of clinical and pre-clinical trials demonstrated their efficacy in treating various diseases [49–51].

A process through which cells take in foreign material by enveloping it with their membrane is known as endocytosis. Pinocytosis and phagocytosis are the two main subtypes of endocytosis. Hormonal receptors, integrins, growth factor receptors, tyrosine

kinase receptors, and lipids are just a few of the proteins that are transported via the critical cellular process known as endosomal trafficking.

Pinocytosis, from the Greek "pino" meaning to drink, is the mechanism through which the cell absorbs liquids and disperses tiny molecules. The cell membrane bends and forms tiny pockets during this process, catching the cellular fluid and other dissolved materials (Figure 3). In many cases, nanodrugs follow this endocytosis (pinocytosis) [52]. Other delivery methods include clathrin-dependent delivery [53,54].

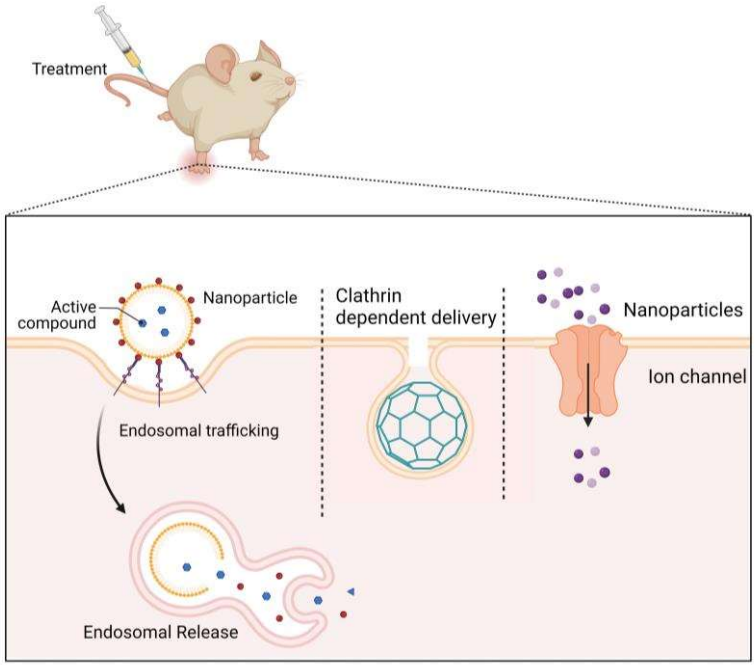

Figure 3. Major cellular uptake methods of nanoparticles (cellular uptake occurs mainly through endosomal trafficking, through clathrin-dependent delivery, and through ion channels).

Biomedical uses of nanohydrogels are wide in drug administration, tissue engineering [55], and wound dressing and healing due to their biocompatibility [56], nontoxicity [57], and high absorption capacity [58]. Furthermore, site-specific targeted drug administration is possible with stimulus response factors such as temperature and pH-dependent upgraded hydrogels [52,59]. There is evidence of the use of nanometal-hydrogel for tissue regeneration [60].

Nanohydrogel molecules have the features of hydrophilic and hydrophobic components, disperse in the solution to form micelles [61]. Micelles are generated by self-assembly, where the process does not begin until a specific minimum concentration is reached. This concentration is frequently referred to as the crucial micellar concentration [62]. Ag-NPs form micelles to be stable in aqueous solutions [59]. Reverse micelles are used for bimetallic (Au/Pd) NP formation [63].

Dendrimers are such structures that have branches or arms like trees and are globular, nanodimensionally compact, and radially symmetric [64]. The capacity of dendrimers to distribute drugs in a regulated and targeted manner is their most promising use. Higher stability, a longer half-life, and greater bioavailability are characteristics of drugs conjugated to such delivery systems. Additionally, prolonged drug release via the drug-dendrimer combination lowers the systemic toxicity and maintains tumor tissue-specific aggregation [65,66].

A significant number of clinical and preclinical studies show how deeply the function of NPs as carriers of therapeutic agents has been studied. NPs are regarded as one of the most promising groups of medication delivery systems. NPs can bind macromolecules such as proteins, antibodies, or nucleic acids and can encapsulate both hydrophilic and

hydrophobic medicines [67]. Paclitaxel has been exemplified in polymeric NPs made by impeding copolymers of mono-methoxy polyethylene glycol and poly-D,L-lactide [68].

Additionally, NPs may be programmed to react to many environmental factors, including pH, light, temperature, enzymes, and other biological and chemical agents. The most often employed of all these stimuli is pH responsiveness. The pH differential can aid in distinguishing tumor tissue (pH 5.7–7.0) from normal tissue (pH 7.4). The capacity to directly release medications at tumor sites has made this pH responsiveness valuable in a variety of cancer and tumor therapies [69].

Inorganic NPs have been studied for their potential biomedical applications in addition to polymeric NPs. There are various ways to make inorganic NPs, including the crystallization of inorganic salts, thermal breakdown, and other well-known synthetic processes [70]. Several inorganic NPs, including Au, Ag, Pt, iron oxide (FeO), cerium oxide (CeO_2), and zinc oxide (ZnO), have been successfully synthesized and used in numerous preclinical and clinical trials. However, because of their higher biocompatibility, higher biodegradability, and lower systemic toxicity, polymeric nanoparticles are preferred over inorganic NPs [71]. Many researchers have been interested in liposomes as a potential medication delivery technology due to their capacity to selectively transport both hydrophilic and hydrophobic medicines to their respective target sites [72].

Liposomes are capable of encapsulating and protecting both hydrophilic and hydrophobic medicines before releasing them at specific sites. Multilamellar vesicles are made up of concentric spheres of phospholipids separated by water layers, while unilamellar vesicles only have a single phospholipid bilayer encapsulating the aqueous solution [50]. Au-NPs enable green synthesis by using glycerol liposomes [73,74] and the selective release of contents from liposomes caused by light [75]. Multifunctional metallic NPs can be formed for medical imaging and micro-fluidity [76,77].

Scaffolds are important in biomedicine and tissue engineering because of their capability to foster cell adhesion, proliferation, and differentiation, all of which are necessary for tissue development. The scaffolding allows cells to develop in all the right places, which results in the production of tissue. A biocompatible matrix is required for optimal cell growth, the strategy of employing scaffolds is of utmost relevance [78,79]. Scaffolds have great biocompatibility, mechanical strength, porosity, and interconnectivity, all of which are necessary for clinical application [80]. There is evidence of a nanohybrid scaffold of glycolic acid-g-chitosan-Pt-Fe_3O_4 being used as a drug delivery system [81].

1.5. Scopes of Metal Nanoparticles in Remedies

To ensure that the human body functions normally, specific levels of certain metals must be present. The main functions of metals are to catalyze certain reactions and act as cofactors or prosthetic groups of enzymes. The required metals for humans include Na, K, Fe, Mg, Zn, Cd, Mn, Cu, V, Cr, Mo, Co, and Ni. In the absence of certain essential metals, anemia could occur [41].

Iron deficiency causes the loss of functional blood proteins such as hemoglobin, myoglobin, etc., whose function is to carry oxygen. Iron deficiency accounts for roughly half of all anemia cases worldwide. As a first-line therapy, oral iron supplementation is recommended; however, IV iron formulation is a recent addition to anemia treatment, and hepcidin could be a future diagnostic target [42]. Vitamin B12 is made of a cobalt complex called cobalamin, and the lack of this vitamin results in pernicious anemia.

Zn is used as a catalyst for various enzymes. Importantly, it is required for red blood cell production. That is why a deficiency in this metal can cause anemia. It can heal wounds, and Zn ions (Zn^{2+}) can be used for treating the herpes virus [82]. According to one study, infant's diets which had low in Zn; had higher rates of copper anemia, which can lead to heart disease also [31]. Copper gluconate, copper chloride, or copper sulfate are used as oral or IV copper supplements in copper anemia [83]. Some potential metallic NPs are shown in Figure 4.

For the treatment of rheumatoid arthritis [84], juvenile rheumatoid arthritis, and psoriatic arthritis, gold salt complexes have been used. Though the mechanism is still uncovered, it is assumed that Au salts interact with albumin and are taken up by the immune cells, causing antimitochondrial effects and the apoptosis of cells [85–87]. Head and neck tumors showed specificity towards the Pt-based compounds; they might work by cross-linking the DNA in tumor cells [88]. For the treatment of manic-depressive disorder, lithium carbonate (Li_2CO_3) is used [89].

To prevent the contagiousness of infection, Ag has been used for various remedies since 4000 BC. The bactericidal effect of silver is well established, and topically, it is used to prevent infection of burned skin; it is also being used for ulcerations, bone prostheses, orthopedic surgery, catheters, heart devices, and surgical apparatus [90].

Diabetes, atherosclerosis, cancer, myocardial ischemia, pulmonary TB, asthma, Alzheimer's disease (AD), and Parkinson's disease (PD) are only a few of the many chronic diseases for which drug delivery vehicles have been extensively studied and shown to be effective. A number of these medicines, including Caelyx®, Abraxane®, Myocet®, Mepact®, Rapamune®, and Emend®, have been marketed for human use after positive results in preclinical and clinical testing. The potential of innovative therapeutic agents, such as peptides, nucleic acids (RNA and DNA), and genes, to be exploited as nanomedicines for the treatment of numerous chronic diseases, has been demonstrated beyond that of medications and chemicals [91].

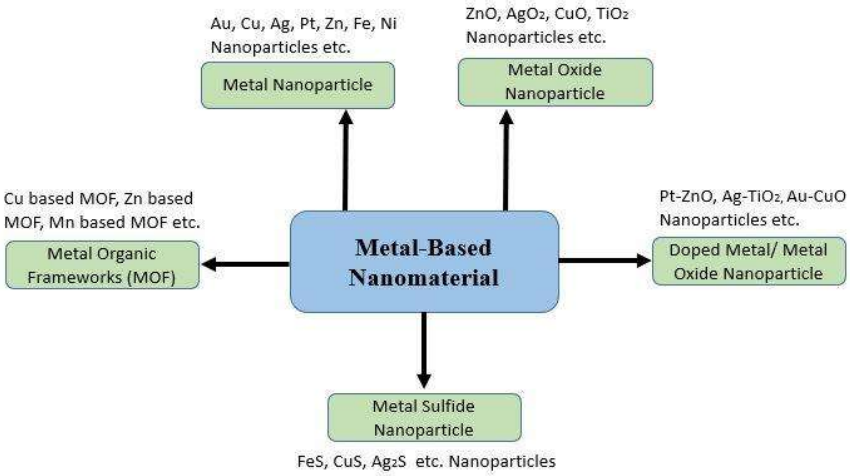

Figure 4. A couple of possible metallic nanoparticles. Adapted with permission from Ref. [91].

NPs based on metals such as Au, Ag, Fe, Cu, Pt, Zn, and so on have attracted a lot of interest in the medical field. NPs of metals have been demonstrated to exist in aqueous solutions, as demonstrated by Faraday [11]. Metallic NPs' hue and structure were analyzed by Kumar et al. [92] many years later. NPs can be manufactured and optimized in the present day by altering the chemical groups that aid in binding the antibodies. Ag-NPs could be utilized to treat a variety of skin ailments. Biomedical applications of noble metal NPs (Au, Ag, and Pt) include cancer treatment, drug transport, radiation therapy augmentation, thermal ablation, fungus elimination, diagnostic testing, and gene delivery, among many others. NPs of noble metals have special qualities that increase their worth. Peptides, antibodies, RNA, and DNA are just some of the functional groups that can be attached to metal NPs to make them more specific to the cells they are intended to target [93]. Some key NPs as well as their physiological applications are summarized below in Table 2.

Table 2. Some applications of metal nanoparticles.

Nanoparticles Name	Site of Action	Application	References
Au-NPs	Cancer gliblastoma-based multiforme	Radiosensitizer applications	[94,95]
Au-NPs	Cancer cell	Radiosensitizer application	[96]
Ag-NPs	Skin	Skin penetration evaluation	[97]
Pt-NPs lined with polyvinyl alcohol	Brain	Toxicity evaluation	[98]
Ag-NPs	Antimicrobial agent	Antimicrobial assessment	[99]
Au-NPs/Ag-NPs	Cancer cell	Photothermal therapy, imaging therapy	[100]
Au-branched shell nanostructure	Breast cell	Imaging therapy, photothermal therapy, chemotherapy.	[101]

1.6. Major Challenges of Using Nanoparticles in Medical Treatment

Firstly, though many testing procedures [102] have been developed for the evaluation of NP toxicity [103], these procedures are not universal for all NPs; they are designed for individual NPs and are not applicable for hybrid NPs. This fact leads to an undesirable outcome from the real objects and could be harmful for the body. As its effect is dependent on the size, shape, surface charging condition, and capping agents, it is really difficult to develop an accurate strategy to find out the toxicity. On the other hand, Au-NPs' effect also depends on its target receptor or organ; for example, different NPs show their effect at different concentrations. Thus, it is urgent to formulate some universal methods, such as good laboratory practice (GLP), to evaluate the safety of the NPs [103–105]. The adsorption of proteins to the particles also correlated with their physical characteristics (size, shape, charge, etc.) [106]. Significantly, metal oxide NPs have a high tendency to produce toxicity, this toxicity can be caused by a variety of mechanisms, including oxidative stress, coordination effects, nonhomeostatic effects, genotoxicity, and others. Size, solubility, and exposure routes all have an impact on metal oxide nanoparticles [107].

Secondly, although Au-NPs show outstanding result in tumor disease, there is a lack of studies to find out its pharmacokinetics (clearance and bio distribution) inside the human body. In vitro and in vivo studies cannot give the full picture of the biodistribution in the organism, which limits the wide use of gold NPs [108].

Third, this study discovered that in the case of tumor treatment, only 0.7% of NPs were able to reach cancer cells, with some exceptions reaching more than 5%. Moreover, when the NPs are injected in the blood circulation, they get absorbed in the mononuclear phagocytic system (MPS) and renal system, which reduces the effectiveness of the MPS day by day.

Finally, because there have been few Au-NP clinical trials, the data do not allow for comprehensive research on clearance, distribution, and protein absorption. Thus, a comprehensive trial for safety and toxicity should be carried out [109].

This review aims to highlight experiments conducted in the path of advancement in the therapeutic use of above discussed six metal NPs, such as Ag, Au, Zn, Cu, Fe, and Ni; additionally, we have used the literature to highlight the possible mechanism of action of significant effects of the selected potential metal NPs.

2. Therapeutic Applications of Metal NPs

2.1. Therapeutic Interventions of Gold Nanoparticles (Au-NPs)

When Robert Koch discovered that gold cyanide had a bacteriostatic effect on Mycobacterium TB, the medical use of gold for the treatment of tuberculosis was established for the first time. This led to the introduction of gold as a medicine in the 1920s [110].

Au-NPs have a tendency to aggregate at tumor sites [95]. Tumor cells can be killed by Au-NPs in a variety of ways, including as drug delivery systems for mechanical damage, anticancer medicines, and photothermal ablation [111].

In particular, Au-NPs are used in drug delivery, imaging, photo-thermal therapy, sensing, catalysis, and antimicrobials [112]. The list of applications of Au-NPs is much longer

because of their unique properties (Table 3). The biocompatibility of gold nanoparticles has been well documented; however, the typical reduction procedures used to create them can leave behind harmful chemical species [113]. Consequently, Au-NPs manufactured in an environmentally friendly manner hold far more promise in a variety of settings. Although Au-NPs are not as widely used as Ag-NPs as antibacterial agents, they nonetheless have considerable impact against a wide range of diseases due to their inherent biocidal qualities [112,114].

Au-NPs of 60 nm showed a positive result in retinoblastoma treatment [115], Au nanopopcorn 28 nm in size is used to diagnose prostate and breast cancer [116], and Au nanostars (Au-NS) 30 and 60 nm in size can be used to identify brain tumors, and this same NP showed a satisfying result against bladder cancer [117].

Silica-coated Au nanorods showed effective antitumor activity, both in vivo and in vitro, against breast cancer by targeting CD44+ receptors [118]. Colloidal Au-NPs are of interest as nontoxic carriers for drug delivery [119–121]. In a study, it was found that the internalization of the 50 nm spherical gold nanoparticles (AuNPs) was the best of all the nanoparticles investigated [122]. TrxR (thioredoxin reductase) function can be inhibited by gold compounds, which causes tumor cells to accumulate reactive oxygen species (ROS) and experience oxidative stress, which ultimately kills the tumor cells [123,124] and the proposed anticancer mechanism of Au-NPs is illustrated in Figure 5.

Nanotherapeutic Application of Gold

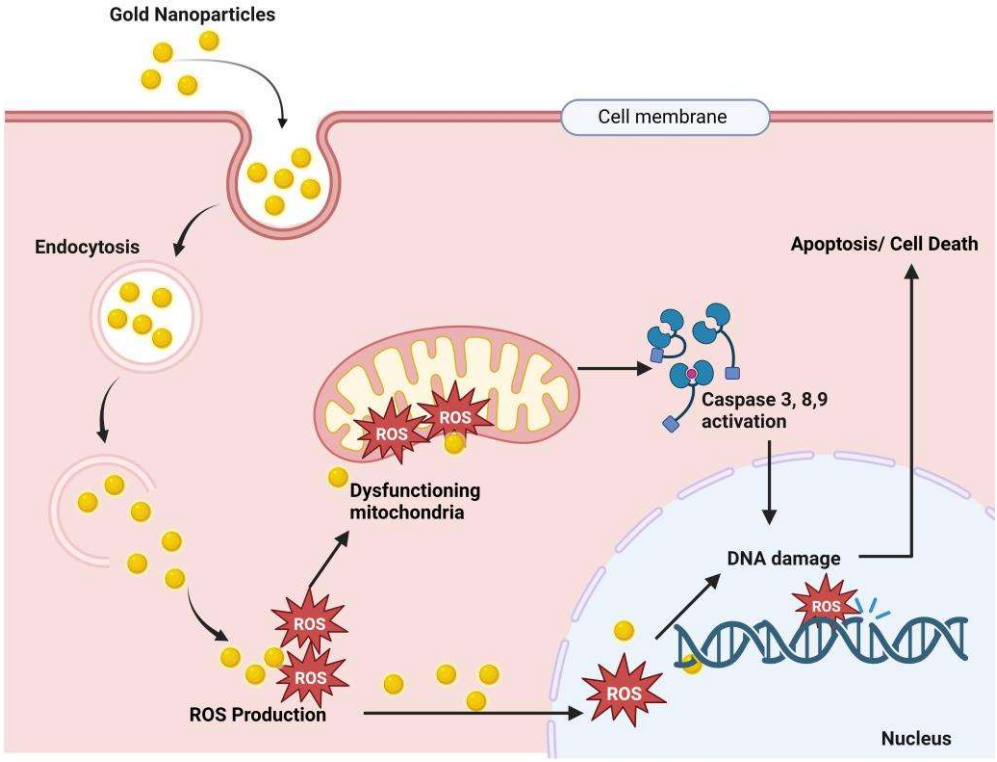

Figure 5. Proposed anticancer mechanism of gold nanoparticles. Here, Au-NPs pass through the cancer cell membrane by endocytosis, and endosomal release causes ROS (reactive oxygen species) production. These ROS cause mitochondrial dysfunction and result in caspase 3, 9, and 8 activations, which results in DNA damage and finally cell death [123–126].

Table 3. Nanotherapy of gold nanoparticles.

Nanoparticles (Diameter)	Test Medium	Concentration	Effect/Result	Disease Against	References
Anticancer Effect					
Au-nanopopcorn (28 nm)	LNCaP (prostate cancer cells)	0.5 mL	Popcorn-shaped Au-NPs enhanced Raman intensity to recognize prostate cancer cells.	Prostate and breast cancer	[105]
Au-NPs	Y79 (MTT analysis)	1.75, 3.5, 7, 14, 28 and 56 µg/mL	Forty-eight hours after applying Au-NPs, 0.5 to 11 min hyperthermia is applied, which shows 50% cell viability after 4.5 min, but without NPs, 9 min is required to obtain same effect.	Hyperthermia in cancer	[115]
Au-NS (30 and 60 nm)	MB49 bladder cancer cell line in mice	0.1 nM	Synergistic immuno photo nanotherapy (SYMPHONY) produce better survival than other groups. In photo thermal monotherapy Au-NPs has much efficiency than nanoshells.	Bladder cancer	[117]
Silica coated Au nanorods	Mammary carcinoma cells	-	Showed efficient in vivo and in vitro antitumor activity in targeting CD44+ receptor.	Breast cancer	[118]
DOX@ Au-NPs (2 nm Au-NPs)	Breast Cancer Cell lines (MCF-7 and MDA-MB-231); Murine Mammary 4T1; CD-1 Mice	5 mg/kg dose	Good renal clearance with fruitful targeting. Decreased normal tissue toxicity with improved antitumor efficacy.	Breast cancer	[119]
PDC-PEG-Au-NPs (25–50 nm GNPs)	Murine lymphoma cells (A20)	Up to 50 µM dose	Half-life of drug increased, toxicity observed in targeted cells, and effective for a long time.	Anticancer	[120]
BLM-DOX-PEG-Au-NPs (13 nm GNPs)	HeLa, cervical cancer cell line	10–100 nM dose	Cancer cell environment-mediated drug release and improve EC_{50}	Cervical cancer	[121]
Au-nanostars (Au-NS) (30 and 60 nm)	Glioblastoma model on mice	0.1 nM	7.2% ID/g uptake of Au-NPs in the brain tumor, which is identified by PET/CT scan.	Brain tumor	[127]
Chitosan/Au-NPs	HepG-2 and Caco-2 cell lines	0.1, 0.05, 0.025, 0.0015 mg/mL	Cancer cell proliferation is inhibited more than chitosan.	Cancer and bacterial infection	[128]
NP-based nucleic acid conjugates Au@GO NP-NACs	Result identified by in vitro microfluidic models. Bcl-2	100 µg/mL of Au-NPs	Better live cancer cell identification by SERS and synergistic and specific killing of cancer cells.	Anticancer	[129]

Table 3. *Cont.*

Nanoparticles (Diameter)	Test Medium	Concentration	Effect/Result	Disease Against	References
Cancer-targeting peptide-functionalized NP (3.52 nm) using Au-NPs (26.2 nm) and TA-peptide complex	MCF-7 and T47D (breast cancer cell lines), on tumor containing mice	-	Targeted cell death by apoptosis. Considerable hemocompatibility, higher release of cytochrome c, and higher antitumor activity is found.	Breast cancer	[130]
Chitosan coated Au-nanospheres	RAW264.7 cells	IC_{50} value 127 μM	This study compares the cellular uptake of Au-NPs and found that Stars < rods < triangles (lowest to highest uptake order). The mechanism of cellular uptake was endocytosis. Au-NP nanorods showed greater cellular uptake and high cytotoxicity against RAW264.7 cells.	Anticancer	[131,132]
Chitosan coated Au-NS		IC_{50} value 81.8 μM			
Chitosan-coated Au-nanorods		IC_{50} value 22.7 μM			
Au-NPs	Osteosarcoma mouse model	-	Au-NPs with CD133 and hyaluronic acid increased the photo thermal antitumor therapy. HA can gourd the photosensitive drugs from photo-degradation and inhibited the proliferation of osteosarcoma cells.	Bone cancer	[133]
Au-NPs covered with multivalent hydrocarbon. (6.9 ± 2.9 nm)	Xenograft mouse model with the HeLa, SCC7, and SKBR3 cancer cell lines	100 nM–10 mM	Tumor growth was considerably suppressed in C18@F127 injected in xenograft mice compared with the control group.	Breast cancer	[134]
Anti-HER2 functionalized Au-on-silica nanoshells	RAW 264.7 cells	LD_{50}: 1 mg/mL and 10 μg/mL for cationic carrier.	Targeted action; precisely eliminating cancer cells while protecting healthy tissues	Breast cancer	[135]
Au-NPs produced from *Enterococcus* sp.	Colorectal tumor cells (HT-29)	5–24 μg/mL	Inducing ROS and caspase-3 expression, weakening the potential of mitochondrial membrane.	Anticancer	[136]
PTX-TNFα-PEG-Au-NPs (32.6 nm)	Ovarian cancer cell line (A2780); B16/F10 tumor induce C57BL/6 mice	2.5 mg/kg dose	Specific delivery of NPs to tumor and improved efficacy	Ovarian cancer	[137]
DOX-PEG-Au-NPs (41 nm Au-NPs)	Ovarian cancer cell line (A2780); CD-1 mice	6 mg/kg dose	Significantly reduced normal tissue toxicity	Ovarian cancer	[138]
CIS-GLC-PEG-Au-NP (20 nm GNPs)	Skin cancer cell line A-431; A-431 cell line bearing mice	10 mg/kg dose; 25 Gy at 6 MV	Same type effect to free cisplatin; improved result when used in combination with radiation	Skin cancer	[139]

Table 3. *Cont.*

Nanoparticles (Diameter)	Test Medium	Concentration	Effect/Result	Disease Against	References
Alginate conjugate with Au-NPs and CIS (44 nm NP)	Cervical cancer cell line (KB)	20 µg/mL dose of Au-NP along with 5 µg/mL CIS; 4 Gy at 6 MV	ACA and radiotherapy found increased efficacy over cisplatin and radiation. Using photothermal therapy further enhanced the anticancer effect.	Cervical cancer	[140]
5-FU/GSH-GNPs (9–17 nm Au-NPs)	Colorectal cancer cell lines (isolated frompatients)	0.5–1.5 mg/mL dose	Better anticancer effect, and minimized the drug doses as a result.	Colorectal cancer	[141]
Cs-Au-NPs-DOX (21 nm GNPs)	MCF-7, Breast cancer cell line	0.05–0.3 mM dose; 0.5, 1, and 3 Gy at 6 MV	Improved test results, decreased survival fraction, upregulated apoptosis, and DNA damage.	Breast cancer	[142]
Au-NP-PEG-RGD; CIS (10 nm Au-NPs with 435 nM CIS)	MDA-MB-231, Breast Cancer Cell line	0.3 nM dose; 2 Gy at 6 MV	Increased efficacy of treatment compared to cicplatin or radiation alone.	Breast cancer	[143]
Au-NP-PEG-RGD; DTX (17.2 nm GNPs)	Breast Cancer Cell line (MDA-MB-231) and Cervical Cancer Cell line (HeLa)	0.2 nM Au-NPs with 50 nM DTX; 2 Gy at 6 MV	Greater retention of Au-NPs due to cell synchronicity induced by DTX. Synergistic therapeutic action observed when Au-NPs and DTX were combined.	Breast cancer	[144]
Antimicrobial Effects					
Gold-chitosan hybrid NPs (16.9 nm)	Tested against the *S. aureus* (Gram-positive) *P. aeruginosa* (Gram-negative) bacteria	0.25 mg/mL	The action is still not clear.	Bacterial infection	[145]
Au-NPs (17 nm)	HIV-1	0.05–0.12 mg/mL	Au-NPs inhibits HIV-1 but its mechanism is unknown.	Viral infection	[146]
Au-NPs (25 nm)	Candida sp	16–32 µg/mL	Cell death for intracellular acidification by the inhibition of H+ ATPase.	Fungal infection	[147]
IgG-Au-NPs (32 nm)	MRSA cultures	1–50 mg/L	6.25% minimum inhibition concentration (MIC) for the Ig-Au-NPs, while 25% MIC was found for Au-NPs alone.	Methicillin-resistant *Staphylococcus aureus* (MRSA) infection	[148]

Table 3. *Cont.*

Nanoparticles (Diameter)	Test Medium	Concentration	Effect/Result	Disease Against	References
Miscellaneous Effects					
Au-NPs/chalcones conjugate (2 to 12 nm)	HEK293 cells	20–100 µg/mL	Therapeutic development of antidiabetic drug, which is derived from *H. foetidum* by increasing glucose uptake and no particle shows cytotoxicity against HaCaT keratinocytes. Helichrysetin is a potential compound for antidiabetic effect.	Antidiabetic	[149]
Au-NPs/chalcones conjugate (2 to 12 nm)	α-amylase and α-glucosidase enzyme	20–100 µg/mL	Potential enzyme inhibitory activities against α-amylase and α-glucosidase enzymes.	Enzyme inhibition	[149]
Au-NPs	pBR322 (plasmid DNA)	64 ng/mL (nanogram)	γ-ray radiation applied by HDR brachytherapy, ROS (reactive oxygen species) formation and DNA breaks occurred in positive charged Au-NPs but not in negative charged Au-NPs.	Plasmid DNA damage	[150]
SPIO-Au-NPs (FeO-Au) core-shell NPs	PC-12 cells (Neuron like cell)	127 µg of SPION-Au-NPs	Shows higher intracellular interaction with PC-12 neuron-like cells.	Neuroregenaration	[151]
Synergistic Immuno Photothermal Nanotherapy (SYMPHONY) 30, 60 nm	Tumor cell treated	0.05 nM NPs with radiation	In murine animal models, it provides a 'cancer vaccine' effect that leads to immunologic memory and inhibits cancer recurrence.	Photoimmunotherapy	[152]
Peptide-coated Au-NPs	Human peripheral blood mononuclear cells	12.5–50 µg/mL	Efficiently suppressed TLR signaling and shielded mice from LPS-induced acute lung injury. PPIs and the recently found that Au-NPs-based TLR inhibitors have comparable modes of action.	Acute Lung Injury	[153]

2.2. Therapeutic Interventions of Silver Nanoparticles (Ag-NPs)

Silver has excellent physicochemical features, such as catalytic, optical, electric, and, of course, antibacterial capabilities, and these qualities make silver nanoparticles the most marketable nanoparticles. In the presence of Ag-NPs, the synergistic impact of antibiotics such as cefotaxime, azithromycin, cefuroxime, chloramphenicol, and fosfomycin against *E. coli* was greatly boosted as compared to antibiotics alone [80].

Other metal NPs may exhibit equivalent efficacy against particular germs, but overall, silver is said to be the most effective material against a variety of pathogens. Ag-NPs inhibit the extracellular activity of severe acute respiratory distress syndrome coronavirus 2 (SARS-CoV-2) [154].

Ag-NPs are the preferred metal when antibacterial characteristics are required. The antibacterial, antiviral, antioxidant, and anticancer characteristics of silver are well recognized, and it has the potential to be developed into a unique therapeutic agent. Ag also has antiparasitic, antiviral, and anticancer qualities [155,156], and the mechanisms of action of these effects are illustrated in Figure 6. Ag-NPs, after entering cells by endocytosis, produce ROS that damage the endoplasmic reticulum and mitochondria. The cellular pathways NF-kB, PI3K/AKT/mTOR, Wnt/beta-catenin, MAPK/ERK, and ERK activation result in DNA fragmentation, cell cycle arrest, and cell apoptosis [157–161]. Table 4 shows the prominent nanotherapeutic applications of silver.

Nanotherapeutic Application of Silver

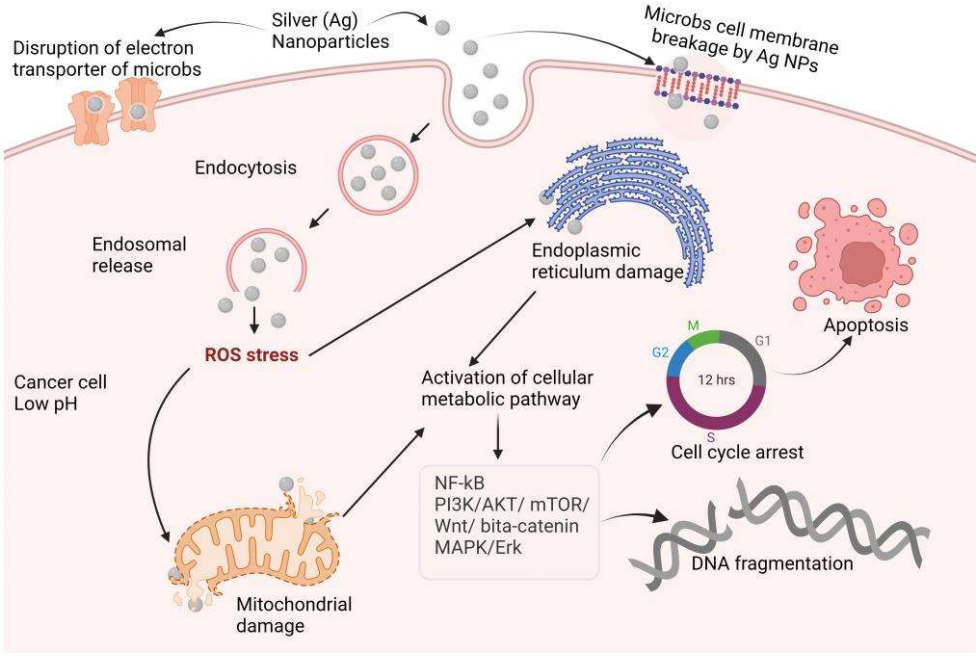

Figure 6. Proposed anticancer mechanisms of silver nanoparticles (NF-kB: nuclear factor kappa-light-chain-enhancer of activated B cells; PI3K: phosphoinositide 3-kinases AKT: protein kinase B; mTOR: mammalian target of rapamycin; Wnt: wingless and Int-1; MAPK: mitogen-activated protein kinase; ERK: extra-cellular receptor kinase).

Table 4. Nanotherapy of some silver nanoparticles.

Nanoparticles (Diameter)	Test Medium	Concentration	Effect/Result	Disease Against	References
Anticancer Effects					
Ag-NPs (5–20 nm)	MCF7-FLV cell line	136 µM	Cytotoxic effects against breast cancer.	Breast Cancer	[70]
Ag-NPs (26.18 nm)	Human alveolar cancer cell line: A549	87 and 41 µg/mL	Activity against the A549 cell line without showing any damage in noncancer cells.	Alveolar cancer	[162]
Ag-NPs (50–70 nm)	Human acute T cell leukemia cell line	10 to 50 µM	Cytotoxic activity against leukemia.	Leukemia	[163]
Ag-NPs (33 nm)	Human cervical cancer cells (HeLa)	10 to 50 µg/mL	Induced cytotoxicity in HeLa cells in a concentration-dependent manner.	Cervical cancer	[164]
Ag-NPs (24–150 nm)	HCT-116 cells colon cancer cell	100 µg/mL	The sub-G1 phases of the cell cycle were changed, and larger levels of fragmented DNA were discovered.	Colon cancer	[165]
Ag-NPs (6 nm) with gemcitabine (GEM)	Human ovarian cancer cell line A2780	50% inhibitory concentration (IC_{50}) of GEM and Ag-NPs after a 24 h exposure was 100 and 90 nM	Lowering cell viability and proliferation, as well as increasing LDH leakage and ROS production.	Ovarian cancer	[166]
Ag-NPs (2.8 and 18 nm)	PANC-1 and hTERT-HPNE	1.67 µg/mL for 2.8 nm size and 26.81 µg/mL for 18 nm size	Ag-NPs triggered programmed cell death in PANC-1 cells, including apoptosis and necroptosis, as well as autophagy and mitotic catastrophe, in a concentration- and size-dependent manner.	Pancreatic ductal adenocarcinoma	[167]
Ag-NPs (60 nm)	MG63 osteosarcoma cell line	81.8 ± 2.6 and 75.5 ± 2.4 µg/mL	Chromatin condensation causes dose-dependent cytotoxicity and ultimately cell death.	Osteosarcoma	[168]
Ag-NPs (lesser than 50 nm)	Pleomorphic hepatocellular carcinoma (SNU-387), hepatic ductal carcinoma (LMH/2A), morris hepatoma (McA-RH7777), and novikoff hepatoma (N1-S1 Fudr) cell lines	477, 548, and 605 µg/mL	In the presence of Ag nanoparticles, the liver malignant cells viability decreased.	Liver cancer	[169]
Ag-NPs (30 to 90 nm)	A431 human skin cancer cells	64.2 µg/mL	Showed a high level of cytotoxicity against the A431 cell line.	Skin cancer	[170]

Table 4. *Cont.*

Nanoparticles (Diameter)	Test Medium	Concentration	Effect/Result	Disease Against	References
Ag-Cys-NPs	Glioma and neuroblastoma cells	100 and 1000 ng/mL	Ag-Cys-NPs is about 10-fold potent than the Cu-NPs for SH-EP 1 cells and Ag-Cys-NPs is 20 folds more potent than Cu-NPs for glioma cells.	Anticancer	[171]
Antibacterial Effects					
Ag-NPs (10 nm)	*Vibrio cholerae*	40 µg/mL	Antibacterial efficacy of microbial GLP-capped Ag-NPs against *V. cholerae*.	Cholera	[172]
Ag-NPs (70 nm)	*Microbacterium tuberculosis*, H37Rv	6.25–50 mM	Mild growth-inhibitory effect.	Tuberculosis	[173]
Ag-NPs (12.62–27.45 nm) with imipenem	*Klebsiella pneumoniae* clinical strain	Concentration below 3 mg/L	The antibacterial properties of AgNPs in conjunction with imipenem were extended against IRKP infection.	Pneumoniae	[174]
Antiviral Effects					
Ag-NPs (10 nm)	SARS-CoV-2	1–10 ppm	Inhibiting extracellular activity of SARS-CoV-2.	COVID-19	[154]
Ag-NPs (30–50 nm)	HeLa-CD4-LTR-β-gal cells, MT-2 cells, human PBMC	3.9 ± 1.6 mg/mL against HeLa-CD4-LTR-β-gal cells, as 1.11 ± 0.32 mg/mL applied against human PBMC, and 1.3 ± 0.58 mg/mL used against MT-2 cells.	HIV particles are turned inactive quickly, allowing for early disruption of the viral replication cycle.	HIV	[155]
Ag-NPs (3.5, 6.5, 12.9 nm)/Ch composite	H1N1 influenza A virus	250 µL Ag NP/Ch composite suspension	Antiviral activity against H1N1 influenza. Provides a concentration-dependent effect.	Influenza	[175]
Ag-NPs (13, 33 and 46 nm)	HSV-1 and HSV-2	2.5 µL	Vero cell infection by HSV-1 and HSV-2 is downregulated in a dose-dependent manner.	Herpes	[176]
Ag-NPs (10 nm)	HepAD38 cell line	5 to 50 µM	Suppressing HBV RNA and extracellular virions generation in vitro.	Hepatitis B	[177]
Ag-NPs (70–95 nm)	*Chikungunya virus* (CHIKV)	31.25 µg/mL	By inhibiting the cytopathic impact, showing excellent efficacy against CHIKV.	Chikungunya	[178]
Ag-NPs (100 nm)	Serotype DEN-2	20 µL/mL	Plaque assay estimates of dengue virus output were lowered.	Dengue	[179]

Table 4. *Cont.*

Nanoparticles (Diameter)	Test Medium	Concentration	Effect/Result	Disease Against	References
Miscellaneous Effects					
Ag-NPs (37 nm)	*Propionibacterium acnes*	3.1 μg/mL	The mechanism of silver colloid particles bactericidal action on bacteria is still being investigated.	Acne	[180]
Ag-NPs (37 nm)	*Malassezia furfur*	25 μg/mL	Antifungal activity was highest against *M. furfur*.	Dandruff	[180]
Ag-NPs (53 nm)	α-amylase and α-glucosidase	54.56 and 37.86 mg/mL	Inhibition of carbohydrate digestion enzymes, for example α-amylase and α-glucosidase, was effective.	Diabetes	[181]
FA-Ag-NPs	Murine macrophage cells (RAW264.7), mice, age: 7–8 weeks.	0.652 nmol/kg	Rheumatoid arthritis treatment was performed by simultaneously M1 macrophage apoptosis and M1-to-M2 macrophage re-polarization.	Rheumatoid arthritis	[182]
Ag-NPs-PADM hydrogel (PADM = porcine dermal extracellular matrix), 5 and 50 nm	Rat, age: 6-month, weight: 200–300 g	20, 50, and 80 μg/mL	In vivo, Ag-NPs-PADM hydrogel enhanced angiogenesis and repaired infected skin defects.	Skin infection defect	[183]
Ag-NPs 20–35 nm	Rat model	Orally administered Ag-NPs concentrations of 175 and 350 ppm	Ag NPs have a gastroprotective effect in rats against ethanol-induced gastric ulcer. Superoxide dismutase (SOD) and catalase (CAT) activities were increased by Ag NPs.	Gastroprotective	[184]

2.3. Therapeutic Interventions of Copper Nanoparticles (Cu-NPs)

Researchers and health care professionals have been drawn to cupric oxide (CuO) NPs for their physical, chemical, high temperature, and photocatalytic capabilities, but most notably for their antibacterial properties [185]. Copper nanoparticles' synergistic activity with amoxicillin, ampicillin, ciprofloxacin, and gentamicin against both Gram-positive and Gram-negative bacteria was investigated, and ampicillin showed comparatively improved activity compared to alone [186]. Cu-NPs inactivate glycosidase to provide an antidiabetic effect, and the study found that Cu-NPs showed an anticancer effect by activating BAX and p53 and by decreasing Bcl-2 expression, which result in apoptosis in cancer [187]. Cu-NPs increase ROS production in bacterial cells and cause bacterial DNA and protein destruction; on the other hand, accumulation of Cu-NPs in the bacterial cell wall causes cell wall disruption [188–194].

The mechanisms underlying these effects are depicted in Figure 7. Other nanotherapeutic applications of copper are presented in Table 5.

Nanotherapeutic Application of Copper

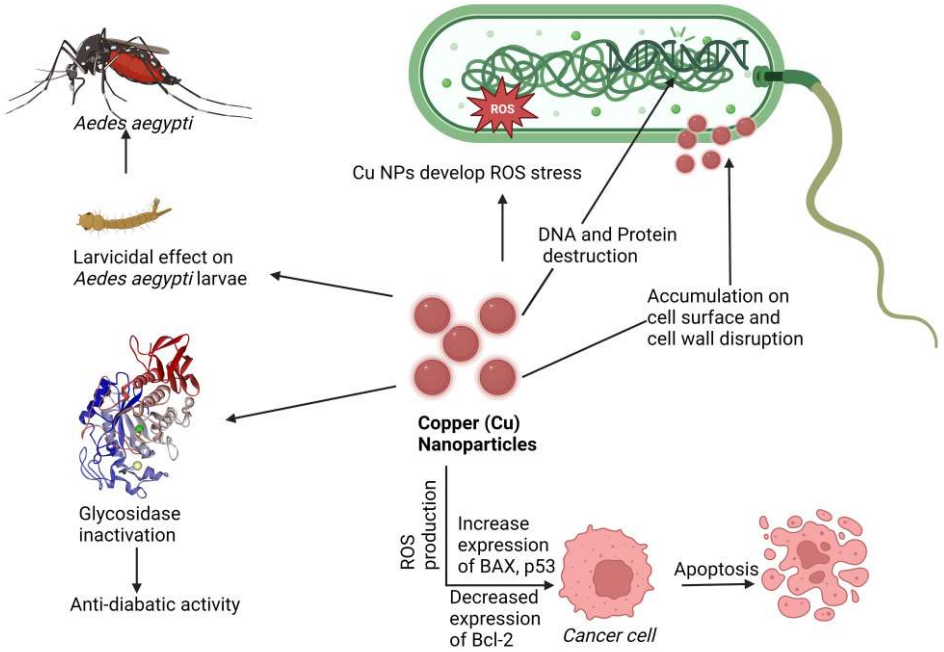

Figure 7. Proposed mechanism of nanotherapeutic applications of copper. Here Cu-NPs showed an anticancer effect by increasing BAX and p53 expression and Bcl-2 downregulating, an antidiabetic effect by glycosidase inactivation, an antimicrobial effect by ROS production cell wall disruption, and a larvicidal effect against *Aedes aegypti* (Dengue virus carrier).

Table 5. Nanotherapy of copper nanoparticles.

Nanoparticles (Diameter)	Test Medium	Concentration	Effect/Result	Disease Against	References
Anticancer Effect					
Cu-NPs/CS-Starch (5–7 nm)	TPC1, BCPAP and FTC133	207 µg/mL	TPC1, BCPAP, and FTC133 cell lines shown substantial antihuman thyroid activity.	Thyroid cancer	[95]
Cu-NPs (62.7 nm) with albumin	MDA-MB 231 cell line	70 µM	Suppressed cancer cell viability while being less harmful to normal cells.	Breast cancer	[190]
Cu-NPs (4.7 to 17.4 nm)	HepG2 cells	19.88 µg	HepG2 cells have a high cytotoxic activity.	Hepatic cancer	[193]
Cu-NPs (4.7 to 17.4 nm)	Caco-2 cells	11.21 µg	Inhibition of Caco-2 cell growth.	Colon cancer	[193]
Cu-NPs (10–20 nm) with chitosan	UM-UC-3 (Transitional cell carcinoma), SCaBER (Squamous cell carcinoma), and TCCSUP (Grade IV, transitional cell carcinoma)	238, 404, and 569 µg/mL	Cytotoxic activity against common bladder cancer cell lines in humans.	Bladder cancer	[195]
Cu-NPs (39.3 ± 5.45 nm)	Human skin carcinoma cells (B16F10) and mouse embryonic fibroblast cell line (NiH3T3)	40 and 120 µg/mL	Mice showed potential suppression of B16F10 melanoma cell proliferation and tumor development inhibition.	Melanoma	[196]
Cu-NPs (12–16 nm)	Human lung carcinoma cells (A549)	20–100 µg/mL	In a dose-dependent way, lung cancer cells showed extensive structural damages and increased oxidative stress indicators.	Lung carcinoma	[197]
Bimetallic CuFe (copper–iron) PBA and CoFe (cobalt–iron) PBA NPs	Tumor tissues for in vitro and BALB/c mice for in vivo test	5, 10, 20, 40, 80, and 160 µg/mL	Prussian blue analogs (PBA-DDSs) prepared with metal NPs doxorubicin (DOX) delivery and pH-controlled release development.	Breast cancer	[198]
Cu-NPs (15 ± 1.7 nm)	HeLa, A549, and BHK21 cell lines	120 µM	Caused the death of tumor/cancer cells through apoptosis.	Antitumor	[199]
Cu-NPs with chitosan (<20 nm)	CHO cells and MC3T3-E1 preosteoblast cells	1–1000 µg/mL	A higher degree of mitochondrial ROS production.	Osteosarcoma	[200]
CuHARS (20–80 nm)	Cell line of a glioma tumor	20 µg/mL	CuHARS decreases the glioma cell and BMVECs viability 20% and 200% respectively. Immune supportive by the production of NO.	Antitumor and immunomodulatory	[201]

Table 5. *Cont.*

Nanoparticles (Diameter)	Test Medium	Concentration	Effect/Result	Disease Against	References
Antiviral Effects					
Cu-NPs (20 nm)	SARS-CoV-2	500 µL	By putting virus-containing media onto copper-coated PP filters and then adding Vero cells, inactivation was assessed.	COVID-19	[189]
Cu-NPs (13.5 ± 0.6 nm)	*Culex quinquefasciatu*, *Anopheles stephensi*, and *Aedes aegypti*	500 µg/mL	A mortality rate that was dosage and time dependent.	Chikungunya	[191]
Cu-NPs (132 nm)	*Aedes aegypti* larvae	55.12 mg/mL	Assessing the larvicidal efficacy of *Aedes aegypti*.	Dengue	[192]
Miscellaneous Effects					
Cu-Epigallocatechin-3-gallate (Cu-EGCG)	Female Sprague rats	50, 100, 200 µg/mL	Inhibited bacteria such as *E. coli* and *S. aureus* to protect from wound infection.	Wound healing	[56]
Cu-NPs (30 and 50 nm)	*Streptomyces griseus*	-	Nanocopper has the potential to be an effective new fungicide.	Red root-rot disease	[185]
Cu-NPs (12–16 nm)	-	10 µg/mL	Inhibitory actions of glycosidase in vitro.	Antidiabetic	[188]
Cu-NPs (100 nm)	*Fusarium equiseti F. oxysporum* and *F. culmorum*	25, 20 and 19 mm	Exhibited antifungal efficacy against *F. oxysporum*.	Crop diseases	[194]
Cu-NPs (spherical 2.88 ± 0.94, triangular 1.27 ± 0.37 and hexagonal 1.81 ± 0.52 nm)	Cultured porcine ovarian granulosa cells	1, 10, or 100 ng/mL	The ability to influence viability, proliferation, apoptosis, and the release of steroid hormones.	Reproductive disorders	[202]
Cu-NPs (17 and 41 nm)	*T. gondii* tissue cysts	0.2 and 0.3 mL/kg and in combined with atovaquone (100 mg/kg)	Infected mice with *T. gondii* had substantial prophylactic effects when combined with atovaquone.	Toxoplasmosis	[203]
CuHARS (polymer-coated copper cystine high-aspect ratio structures); 60–100 nm	*Escherichia coli* and *Staphylococcus epidermidis*	5 µg	NO production facilitates antimicrobial action of CuHARS.	Antibacterial	[204]

Table 5. *Cont.*

Nanoparticles (Diameter)	Test Medium	Concentration	Effect/Result	Disease Against	References
CuO.MBGs; Mesophorus bioactive glasses (MBGs) (10–20 nm)	In vitro simulated body fluid (SBF)	5% of CuO NPs in MBG	Outstanding biomaterial for bone regeneration. MBGs released therapeutic amounts of Ca^{2+} and Cu^{2+} ions.	Bone defect	[205]
CuS incorporated hyaluronic acid (injectable hydrogel); average 35 nm	SD male rats; weight range 200∼220 g	200, 100, 50, 20, and 10 µg/mL	Improved wound healing and angiogenesis occur.	Wound healing	[206]

2.4. Therapeutic Interventions of Zinc Nanoparticles (Zn-NPs)

Zinc is a material that is frequently used in biomedical applications due to its unique features, such as electric conductivity, optical capabilities, and piezoelectric qualities [207]. Beyth et al. defined the method of killing bacteria using zinc oxide (ZnO) NPs as having two pathways of action [208]. The first involves cell wall penetration, and the second includes the formation of ROS. Zn-NPs follow the Bcl-2/BAX/BAK pathway to cell apoptosis by caspase-3 and -9 and ROS-induced DNA fragmentation leading to cell cycle arrest and apoptosis, and also follow the mitochondrial disruption for an anticancer effect [209–211], as shown in Figure 8.

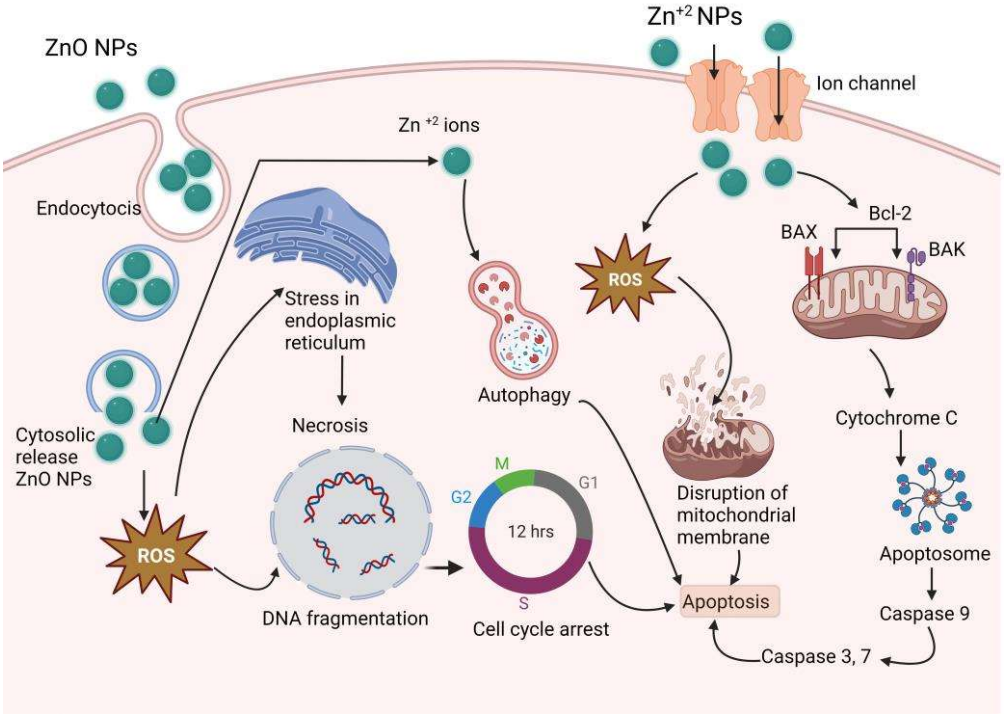

Figure 8. Proposed anticancer mechanism of Zn-NPs (ZnO-NPs create stress in endoplasmic reticulum, and produce ROS, which results DNA fragmentation and cell cycle arrest; on the other hand, produced ROS disrupts mitochondrial membrane and activates caspase 3, 7, and 9, which results in apoptosis).

ZnO-NPs have antibacterial, antifungal, anticancer, antidiabetic, and antitubercular activity, and breast cancer inhibition is an optimistic property that this study observed in a number of studies (presented in Table 6). Even 100 nm Zn-NPs supplemented at 30 ppm improved growth and serum glucose levels in layer chicks [212].

Nanotherapeutic Application of Zinc

Table 6. Nanotherapy of some zinc nanoparticles.

Nanoparticles (Diameter)	Test Medium	Concentration	Effect/Result	Disease Against	References
Anticancer Effects					
ZnO-NPs (16–19 nm)	Breast cancer cell (MCF7), and Lung Cancer cell (A549)	31.2 µg/mL	The cell viability is reduced by NPs, which induces cytotoxicity in cancerous cells.	Anticancer	[213]
ZnO-NPs (100 nm)	Human Breast Cancer (MCF-7) cells	10 µg/mL	Apoptosis is provoked and induced through an intrinsic mitochondrial pathway, depending on caspase activation.	Anticancer	[214]
ZnO (36.91 ± 1.21 nm), ZnO@Ce6 (47.75 ± 0.05 nm) and ZnO@Ce6-PDA (51.92 ± 1.96 nm)	HeLa cells	30 µg/mL	Photothermal and photodynamic action, and increased the cell viability by more than 90%.	Anticancer	[215]
ZnO-NPs (30.4–40.8 nm)	MCF-7 cell line; (Breast cancer cell line)	25 µg/mL	The growth of Gram-positive *Bacillus licheniformis* is inhibited, reducing the viability of MCF-7 cells.	Breast cancer	[216]
ZnO-NPs (30.4–40.8 nm)	MCF-7 cell line; (Breast cancer cell line)	25 µg/mL	The growth of Gram-positive *Bacillus licheniformis* is inhibited, reducing the viability of MCF-7 cells.	Breast cancer	[216]
ZnO-NPs (66.25 nm)	MDA-MB 231 and MCF-7 breast cancer cell lines.	0.1, 0.05 and 0.01 M	The activity of MDA-MB 231 cells is inhibited with increased concentration.	Breast cancer	[217]
ZnO-NPs (10–15 nm)	MCF-7 cell lines	15.88 µg/mL	Inducing apoptosis in MCF-7 cell line via the Caspase-8 and p53 pathway. Cancer cells may develop and spread throughout the body as a result of mutations (changes) in the p53 gene.	Breast cancer	[218]
PBA-ZnO (<40 nm)	MCF-7 cell lines	35 and 50 µg/mL	Cell death by apoptosis was induced in the MCF-7 cell line by enhancing oxidative stress and mitochondrial damage.	Breast cancer	[219]
ZnO-NPs (10–70 nm)	MCF-7 cell lines	50 µg/mL	Inhibiting apoptosis.	Breast cancer	[220]
Zn-Fe_2O_4-NPs (17.12 nm)	MCF-7 cell lines	25–500 µg/mL	Decrease in cell viability by cytotoxic activity.	Breast cancer	[221]

Table 6. *Cont.*

Nanoparticles (Diameter)	Test Medium	Concentration	Effect/Result	Disease Against	References
ZnO-NPs (31.5 nm)	MCF-7, MDA-MB-231, and HFF cell lines.	11.16 µg/mL	Reduction of the expression of micro-RNAs.	Breast cancer	[222]
Triton-X modified ZnO-NPs (13.45 ± 1.42 nm)	Breast cancer cell line (MDA-MB-231) and normal cell line (NIH 3T3) were used.	55.24 µg/mL	Cytotoxicity is enhanced through surface modification.	Breast cancer	[223]
PEG-ZnO-NPs (150 nm)	DMEM medium (HiMedia)	6.25–37.5 µg/mL	The impairment of DNA damage repair enzyme NEIL2 by inducing apoptosis in breast cancer cells through ROS.	Anticancer	[224]
MSN-ZnO-Au-NPs (76.5 ± 11.8 nm)	Breast cancer cells (MCF-7: estrogen receptor-positive, CAL51: triple-negative).	25 µg/mL	The viability of all cell lines is reduced.	Resistant breast cancer	[225]
ZnO-NPs (12–14 nm)	MDA-MB 231 cancer cells.	7.103 µg/mL	Decreasing cell viability by cytotoxic impact.	Breast cancer	[226]
ZnONPs (25–40 nm)	Michigan Cancer Foundation-7 [MCF7], and murine (TUBO) breast cancer cell lines	8, 4, and 2 µg/mL	Inducing apoptosis by increasing the concentration of ZnO-NPs.	Antitumor	[227]
Zn-NPs (9–17 nm)	MCF-7 (breast carcinoma cell line), HCT-116 (colon carcinoma cells)	3.9, 7.8, 15.6, 31.25, 62.5, 125, 250 and 500µg/mL were used.	For MCF-7, concentrations of 373 µg/mL and >500 µg/mL and for HCT-116, concentrations of 226 and 317 µg/mL were found effective in the in vitro test.	Antitumor	[228]
Antibacterial Effects					
ZnO-NPs (2–28 nm)	*Psedomanas* sp., *Fusarium* sp.	0.1 M	Bacterial membranes are disrupted by the formation of ROS, for example superoxide and hydroxyl radicals.	Bacterial and fungal infection	[229]
ZnO-NPs (45–150 nm)	*Helicobacter pylori* and human mesenchymal stem cells (hMSc)	3.125–100 µg/mL	Biocompatibility to hMSC and described as safe in mammalian cells and can be used as antibiotics.	Antibacterial	[230]
RF-contained Zn^{2+} ion-cross-linked SA-g-AA-M PNPs. <300 nm	Vero cells	100 µg/mL	The gene transcription is inhibited by inhibiting the β-subunit of the bacterial RNA polymerase.	Tuberculosis	[231]

Table 6. *Cont.*

Nanoparticles (Diameter)	Test Medium	Concentration	Effect/Result	Disease Against	References
ZnO-NPs (125 nm)	*Streptococcus mutans*	3.90–4000 µg/mL	Bacteriostatic and bactericidal effects.	Microbial infection	[232]
ZnO-NPs (12 nm)	*Staphylococcus aureus* and *Escherichia coli*	5.6 µg/mL	The ROS production was increased, while the cellular function and cell membrane were disrupted.	Bacterial infection	[233]
MgZnO-NPs/PU (52.65 ± 2.58 nm)	*E. coli*, DH5α strain	9×10^{-5} CFU/mL	The damage of the structure and function of cell originals (mesosome), consequently affecting the deoxyribonucleic acid (DNA) replication by promoting ROS.	Bacterial infection	[234]
ZnO-NPs (20–45 nm)	Ciprofloxacin	500, 1000, and 2000 µg/mL	Increasing antimicrobial activity of ciprofloxacin.	Bacterial infection	[235]
ZnO-NPs (80.1–90 nm)	*Staphylococcus aureus*, *Salmonella Typhimurium*, *Bacillus cereus* and *Pseudomonas aeruginosa*	0.05 and 0.5 mg/L	ZnO NP_S were used in packaging that increased safety against microbes as well as food shelf-life by inhibiting bacterial growth.	Bacterial infection	[236]
ZnO-NPs (30 nm)	*Campylobacter jejuni*	0.025, 0.03, 0.04, 0.05, and 0.10 mg/mL	Damaging membrane integrity by increasing cell membrane permeability.	Bacterial infection	[237]
ZnO-NPs (60–70 nm)	*S. aureus* and *P. aeruginosa* and standard strain of *E. coli*.	1028, 516, 256, and 125 µg/mL were used.	Producing of reactive oxygen species (ROS) is caused disruption of bacterial membranes.	Bacterial infection	[238]
ZnO-NPs (≈66 nm)	Eel kidney cell line (EK-1).	15.75, 31.5, and 3.15 µg/mL	Decreasing cell viability and growth rate of microorganism.	Microbial infection	[239]
ZnO-NPs (15 nm)	*S. pneumoniae*	12 µg/mL	Reducing in microbial biofilm formation.	Bacterial infection	[240]
Antifungal Effects					
ZnO-NPs (12–14 nm)	Aspergillus and Penicillium	5, 10, 15, 20, and 25 g/mL	Cell membrane is damaged and growth rate is inhibited by interaction of zinc ion with cell membrane.	Fungal infection	[226]
ZnO-NPs (35–129 nm)	*Candida parapsilosis*	15.65 µg/mL	Growth is inhibited and surface damage is pronounced.	Fungal infection	[236]
ZnO-NPs (70 ± 15 nm)	*Botrytis cinerea* and *Penicillium expansum*	0, 3, 6, and 2 mmol/L	Fungal hyphae is deformed, while development of conidiophores and conidia are prevented.	Fungal infection	[241]

Table 6. *Cont.*

Nanoparticles (Diameter)	Test Medium	Concentration	Effect/Result	Disease Against	References
ZnO-NPs (430 nm)	*Candida albicans*, *A. niger* and *A. terreus*.	30, 60, and 90 µL	Leading to the death of fungal hyphae by deforming of fungal hyphae.	Candidiasis, athlete's foot, mycosis, and ring worm	[242]
ZnO-NPs	*Candida albicans*	5, 10, 15, and 20 mg/mL	Producing reactive oxygen species (ROS), for example hydrogen peroxide, superoxide anion, hydroxyl radical, and hydroxyl ion.	Fungal infection	[243]
ZnO-NPs (76.15 nm)	*Alternaria alternata*, *Botrytis cinerea*, *Aspergillus niger*, *Penicillium expansum*, and *Fusarium oxysporum.*	256 µg/mL	Disruption of fungal membrane and inhibition of fungal growth.	Fungal infection	[244]
ZnO-NPs (27 ± 5 nm)	*Aspergillus flavus* and *Aspergillus niger*	25 µg/mL	Inhibiting the growth of fungus.	Fungal infection	[245]
ZnO-NPS (60 nm)	*Trichophyton mentagrophyte*, *Microsporum canis*, *Candida albicans*, and *Aspergillus fumigatus*	40 mg/mL	Inhibiting the growth of fungus.	Ring worm	[246]
ZnO-NPs (≤50 nm)	*Aspergillus fumigatus* Fungus and *Candida Albicans*	3, 6, and 12 mL/L	Lowering the growth rate of fungus.	Fungal infection	[247]
ZnO-NPs (13.92 nm)	*Alternaria alternata*	20–160 mg/L	The mycelia growth is inhibited.	Early blight disease	[248]
CS–Zn-CuNCs (16.6–100 nm)	*A. alternata*, *R. solani*, and *B. cinerea*	90 µg/mL	Inhibiting growth by in vitro application.	Fungal infection	[249]
Antidiabetic Effects					
ZnO-NPs (≤10 nm)	Streptozotocin-induced type 1 and 2 diabetic rats	1, 3, and 10 mg/kg	Glucose tolerance was improved, higher serum insulin (70%) and blood glucose (29%) was reduced. Nonesterified fatty acids and triglycerides was also reduced.	Diabetes	[250]
ZnO-NPs (80–100 nm)	Diabetic rats	1, 3, and 10 mg/kg	Glucose disposal, insulin levels, and zinc status are increased.	Diabetes	[251]
ZnO-NPs (10 to 20 nm)	Alpha-amylase	13.085434 µg/mL	The activity of α-amylase is inhibited.	Diabetes	[252]
ZnO-NPs (<100 nm)	Mice	8 and 14 mg/kg	Decreasing blood glucose.	Diabetes	[253]

Table 6. *Cont.*

Nanoparticles (Diameter)	Test Medium	Concentration	Effect/Result	Disease Against	References
ZnO-NPs (22.6 nm)	Wistar rats	70 mg/kg	Hyperlipidemia is controlled through lowering the levels of lipids and lipoproteins in the blood plasma.	Diabetes	[254]
ZnO-NPs	Albino rats	10 mg/kg	Ameliorative effect.	Diabetes	[255]
Miscellaneous Effects					
Zn-NPs (1–100 nm)	Layer chicks	30 ppm	Increasing the level of serum glucose and alkaline phosphate, while decreasing alanine transferase.	Increased chicken growth rate	[212]
ZnO-NPs (48.2 nm)	*Xanthomonas oryzae*	16.0 µg/mL	The bacterial membrane is collapsed and ruptured by interacting with ZnO NPs and as a result in the leakage of bacterial cytoplasm.	Leaf blight	[256]
ZnO-NPs (≤40 nm)	Rats	10 mg/kg	Heart injury is induced by ionizing radiation (IR).	Cardiovascular disorders	[257]
Zn-NPs (50–100 nm)	*Swiss albino* rats	10 mg/kg	Controlling blood glucose level.	Testicular diabetic complications	[258]
Vacuoles-ZnAA-NPs (AA = ascorbic acid)	B16F10 (KCLB 80080) cells. Used African–American, Asian, White donors' tissues.	ZnAA-Vac treated for 12 days at 100 and 1000 ppm	It had a stronger depigmenting impact, reducing the melanin hue by 75%.	Melanin treatment	[259]

2.5. Therapeutic Interventions of Nickel Nanoparticles (Ni-NPs)

Ni-NPs have anticancer action [260,261]. A complex structure of Qu–PEG–NiGs (48–72 nm), green synthesized by *Ocimum sanctum* leaf extract, showed mitochondrial-mediated apoptosis against the MCF-7 cell line [262], antimicrobial activity, antioxidant action, and activity against human ovarian cancer, liver and spleen injury [260,263–265], lung inflammation [266], human lung cancer [267], lymphatic filariasis [268], and larvicidal parasitic activity [269]. Bacterial protein leakage induced by ROS activation [270] and disruption of the cell membrane [271] is one way of causing bacterial cell death. The antimicrobial mechanism is shown in Figure 9. It has numerous other therapeutic properties in a single formulation or a complex formulation, as shown in Table 7.

Nanotherapeutic Application of Nickel

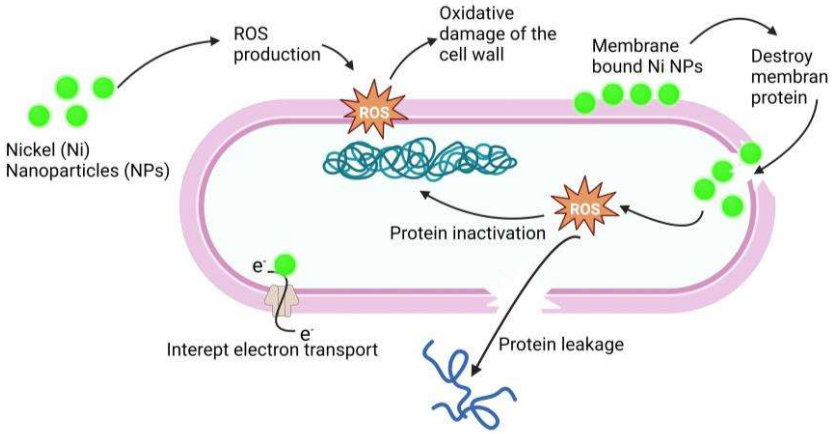

Figure 9. Antimicrobial mechanism of action of Ni-NPs. Ni-NPs cause ROS production that cause oxidative damage of the cell wall and destroy the membrane. ROS cause protein leakage and interrupt electron transport; these processes result in the antimicrobial effect of Ni-NPs.

Table 7. Nanotherapy of nickel nanoparticles.

Nanoparticles (Diameter)	Test Medium	Concentration	Effect/Result	Disease Against	References
Anticancer Effect					
DPMC-Ni-NPs (55 nm)	MCF-7, HepG2, A549, NHDF, and MTT cell lines	25, 22.47, 25.11 and 64.23 µg/mL concentration were used.	Cytotoxicity against breast cancer cell line (MDA-MB-231) was concentration dependent.	Breast cancer	[224]
Ni-NPs (1–100 nm)	Leukemia cancer cells	-	Increasing cell membrane permeability and promoting intracellular absorption in cancer cells.	Anticancer	[261]
Qu–PEG–Ni-NPs (48–72 nm)	MCF–7 cells	6.25 and 50 µg/mL	Mitochondrial-mediated apoptosis is induced through ROS overproduction.	Breast cancer	[262]
Ni-NPs@F. officinalis (16.85–49.04 nm)	PA-1, SK-OV-3, Caov-3, and SW-626 cell lines were used	375, 225, 246, and 279 µg/mL	Reducing viability of malignant ovarian cell line.	Ovarian cancer	[265]
NiO-NPs (5.46 nm)	Human lung cancer cell line (A549)	93.349 µg/mL	Cytotoxicity is exhibited.	Lung cancer	[267]
Nickel-Ferrite ($NiFe_2O_4$) nanorod, rosemary leaves used to prepare NPs, 40–200 nm	Human breast cancer (MCF-7) cell lines were used.	2, 4, 8, 16, 32, 64, 128, 256 and 512 µg/mL	$NiFe_2O_4$ NP had cytotoxicity effect on MCF-7.	Anticancer	[272]
Antibacterial Effects					
Ni-NPs (30 nm)	*Pseudomonas aeruginosa*, *Staphylococcus aureus*, and *Klebsiella* sp.	2.5, 5, 10, 15 and 20 µg/mL	Penetrating the bacteria and damaging them by interacting with phosphorous- and sulphur-containing compounds such as DNA.	Bacterial infection	[263]
NMMNPs (300 to 800 nm) *(NMMNPs = nickel magnetic mirror nanoparticles)*	*S. aureus* and *E. coli* in *S. aureus*	0.01 g	Bacterial growth is inhibited and bacteria are killed.	Bacterial infection	[264]
NiGs-NPs (12–36 nm) Gs:green synthesized	*K. pneumoniae*, *E. coli*, *S. typhi*, *B. subtilis*, and *S. epidermidis*	25–100 µg/mL	Induced ROS generation.	Bacterial infection	[270]
Ni-NPs (0.5 nm)	*Staphylococcus aureus*, *Klebsiella pneumoniae*, *Pseudomonas aeruginosa*, *Vibrio cholerae*, and *Proteus vulgaris*.	1–0.125 mg/mL	Microbial growth inhibition.	Bacterial infection	[273]
Ni-NPs (40–80 nm)	*Escherichia coli*	21, 29 and 36 µM	Growth is inhibited.	Bacterial infection	[274]

Table 7. *Cont.*

Nanoparticles (Diameter)	Test Medium	Concentration	Effect/Result	Disease Against	References
Ni-NPs (10 nm and 50 nm)	*Staphylococcus aurous* and *Escherichia coli* were used.	0.42 and 0.21 µg/mL, 0.84 and 0.42 µg/mL	Destroyed bacterial cells.	Bacterial infection	[275]
Ni-NPs (<100 nm)	*S. aureus* and *Escherichia coli*	0.05, 0.1, and 1 mg/mL	Inhibited the growth of bacterial bioflim.	Bacterial infection	[276]
Miscellaneous Effects					
DPMC-Ni-NPs (55 nm)	DPPH, hydrogen peroxide, and super oxide	-	-	Oxidative stress	[260]
Ni-NPs@F. officinalis (16.85–49.04 nm)	DPPH free radicals	253, 145, and 107 µg/mL	DPPH is inhibited by adding radical species.	Oxidative stress	[265]
Ni-NPs (50 nm)	Sprague Dawley rats	1, 10, and 20 mg/kg concentrations were used.	Increasing number of WBC.	Liver and spleen injury, lung inflammation	[266]
NiO-NPs (5.46 nm)	α-amylase enzyme	268.13 µg/mL	Inhibited α-amylase enzyme and produced a hypoglycemic effect.	Diabetes	[267]
Ni-NPs (80–100 nm)	*Culex quinquefasciatus*.	250, 500, and 1000 ppm	Larvicidal effect.	Lymphatic filariasis	[268]
Ni-NPs (150 nm)	Larvae of *R. (B.) microplus*, *H. a. anatolicum*, *C. quinquefasciatus*, *A. subpictus*, and *C. gelidus*.	10.17, 10.81, 4.93, 5.56, and 4.94 mg/L	Caused larvae death.	Parasitosis	[269]
$NiFe_2O_4$/C nanocomposite.	In vitro: C540 (B16/F10) cells; in vivo: mice model (intratumorally injected)	1.0-MHz radiation was applied with 100 µg/mL NPs	NPs and radiation can recover tumor cells and necrosis, up to 60%.	Sonodynamic therapy	[277]
NiO-NPs preparation with Neem leaf extract. (12 nm)	*S. aureus* and *E. coli*	-	Antibacterial effect was found concentration dependent.	Antibacterial	[278]
$NiFe_2O_4$ nanoparticles (chitosan- and PEG-coated nickel ferrite), 2–58 nm	Mössbauer spectroscopy	Temperature value from 200–800 °C	Hyperthermia heating requires specific particle size, shape, magnetism, and solution concentration.	Hyperthermia heating	[279]
Nickel silicate nanoplatforms (LNS NPs)	Mouse model	-	LNS NPs may produce enough superoxide radicals when exposed to a 660 nm laser; it may simultaneously form oxygen and create superoxide radicals ($O_2^{-\bullet}$).	Hypoxic tumor therapy	[280]

2.6. Therapeutic Interventions of Iron Nanoparticles (Fe-NPs)

Among the Fe-NPs, prominently used NPs include magnetite (Fe_3O_4), hematite, or iron (III) oxide (Fe_2O_3), and the less abundant iron (II) oxide (FeO) [281]. Magnetite (Fe_3O_4) NPs are used in biomedical applications due to their magnetic characteristics, biocompatibility, and, in particular, their superparamagnetic capabilities [282].

Magnetic NPs, also known as superparamagnetic iron oxide, are used in drug delivery [283,284] and hyperthermia therapy [285–287]. Magnetite NPs can produce receptive oxygen species (ROS), which kill microbes, making them a promising contender for an antimicrobial agent. Lung cancer cells terminated by ferroptosis as a result of Zerovalent Fe-NPs (ZVI-NPs) induce mitochondrial malfunction, intracellular oxidative stress, and lipid peroxidation; here, AMPK/mTOR activated by ZVI-NPs cause upregulation of GSK3/β-TrCP, which results in NRF2 degradation and ultimately results ferroptosis, which causes cancer cell damage [288–292], as shown in Figure 10.

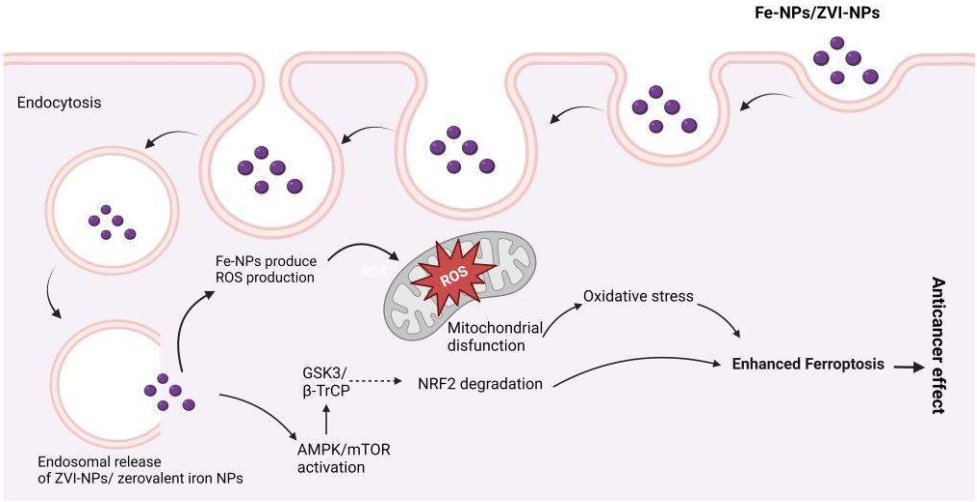

Figure 10. Possible anticancer mechanisms of iron (Fe) nanoparticles (zerovalent Fe-NPs cause ROS production, AMPK/mTOR activation, NRF2 degradation by GSK3/β-TrCP, and mitochondrial disfunction, which results in ferroptosis.

Superparamagnetic iron oxide nanoparticles (SPIONs) provide action against the human breast cancer cell MCF7 [284]. Different nanotherapeutic studies of Fe-NPs are arranged in Table 8.

In the treatment of different types of cancer, ferroptosis, a new Fe- and ROS-dependent form of controlled cell death, has received a lot of attention. The potential of ferroptosis in combination with NPs for cancer therapy is becoming more and more clear as a result of the development of nanomaterials [293]. After cells consume Fe-based NPs, an excess of iron ions released from the lysosome in an acidic environment activates the fenton reaction, which causes ROS formation and cell ferroptosis [294].

Importantly, when antibiotic drugs are coupled with the iron nanoparticles of neem extract, the dose of traditional antibiotics can be decreased by nearly half without affecting efficiency. As a result, the use of natural antibiotics aids in the reduction of regular antibiotic doses [295]. There was also a trial of producing bimetallic NPs (Ag-Fe) that established the synergistic antibacterial (bactericidal) impact of the two metals forming the bimetallic nanoparticles when compared to the effects of the monometallic nanoparticles against yeast and both Gram-positive and Gram-negative multidrug-resistant bacteria [296].

Nanotherapeutic Application of Iron

Table 8. Nanotherapy of Fe-NPs.

Nanoparticles (Diameter)	Test Medium	Concentration	Effect/Result	Disease Against	References
Anticancer Effects					
Superparamagnetic iron oxide nanoparticles (SPIONs (7.3, 15.1, and 30.0 nm	Human breast cancer cell MCF7	80 µg/mL	Higher measurements and more reasonable size of SPIONs upgraded the take-up sum into MCF7 cells.	Breast cancer	[162]
SPIONs	Liver cancer cells (HepG2) (in vitro)	100 µg/mL	A potent cytotoxicity on HepG2 under hyperthermia condition.	Cancer	[287]
Zero valent iron NPs (ZVI-NPs) (97.1–55.77 nm)	BALB/c mice, age: 5–6 week	5 and 10 µg/mL	Lung cancer cells died by ferroptosis as a result of ZVI-NP-induced mitochondrial malfunction, intracellular oxidative-stress, and lipid-peroxidation.	Lung cancer	[288]
CA-coated Fe_3O_4 NPs (50 nm)	4T1 cells	10 µg/mL	Induced tumor cell ferroptosis.	Breast cancer	[297]
SPION-deferasirox	AS1411 DNA aptamer	100 mg	In vivo tumor growth inhibitory effect.	Antitumor	[298]
Rosemary-Fe-NPs (100 nm)	4T1 and C26 cancer cell lines	3.12 to 200 µg/mL	Rosemary-Fe-NPs exerted more cytotoxic effect.	Anticancer	[299]
CAP and iron oxide-based magnetic NPs (MNPs)	A549 cells in vitro	50 emu/g	Potentially inhibited tumor growth.	Lung cancer	[300]
SPIONs (44.6 nm)	Breast cancer cell lines T-47D, BT-474, MCF7, and MDA-MB-231	25, 50 and 75 µg/mL	Extremely moderate molecule take-up and low cytotoxicity, while SPIONLA meaningfully affected cell take-up and cell harmfulness.	Breast cancer	[301]
Fe_3O_4@PEI-Pt(IV)-PEG-LHRH@siEZH2 nanoparticles	A2780/DDP cells (cisplatin resistant)	0.78 to 50 µM	Killing performance to A2780/DDP cells.	Anticancer	[302]
34DABA coated SPIOs (less than 20 nm)	HepG2 liver cancer cells	5, 10, 15, 20, and 25 µg	Good cytocompatibility and higher killing efficiency.	Liver cancer	[303]
Fe-NP nanopowder (35–45 nm)	PC12 cell nervous system (in vitro)	100 µg/mL	Fe-NPs induced apoptotic cytotoxicity.	Cancer	[304]

Table 8. *Cont.*

Nanoparticles (Diameter)	Test Medium	Concentration	Effect/Result	Disease Against	References
Au-Fe_3O_4 -NPs (20.8 nm)	MCF-7 cells	50 µg/mL	Effective and promising photothermal therapy.	Breast cancer	[304]
Iron oxide nanoparticles (Fe_2O_3-NPs) (20 to 60 nm)	Lung cancer cell (A549) lines	Highest concentration of adsorbent (50 mg/L)	No toxicity against A549 cell lines.	Lung cancer	[305]
Miscellaneous Effects					
Magnetic Fe_2O_3-NPs (50–110 nm)	*S. aureus*	DMF arrangement with 40 and 60 MJ laser fluencies showed the most noteworthy antibacterial action.	ROS disrupting bacterial cell membrane.	Bacterial infection	[289]
Fe_2O_3-NPs (10–15 nm)	A/Puerto Pico/8/1934H1N1 influenza virus strain (PR8-H1N1)	1.1 pg	Inactivation of cell protein through the communication of nanoparticles and -SH bunch (proposed, not examined at this point).	Viral infection	[291]
Fe_2O_3-NPs (10–15 nm)	H1N1 Influenza A	4.25 ± 0.2 pg	Change in viral RNA transcripts within 24 h, eight-fold reduction when treated with iron oxide.	Viral infection	[291]
Fe_2O_3-NPs (10–30 nm)	*Trichothecium roseum*, *Cladosporium herbarum*, *Penicillium chrysogenum*, *Alternaria alternate*, and *Aspergillus niger*	0.063–0.016 mg/mL	Development of ROS, protein and DNA damage oxidative stress was the way of producing antifungal effect.	Fungal infection	[292]
Zero-valent iron (Fe0) NPs, spherical (31.1 nm)	*Staphylococcus aureus* (Gram-positive) and *E. coli* (Gram-negative)	MIC at 30 µg/mL and complete growth inhibition concentration at 60 µg/mL	Oxidative stress generation via ROS and visible damage to bacterial protein and DNA.	Bacterial infection	[298]
4 nm core Fe_2O_3 coated with tartaric/adipic acid	Mitochondrial DNA (mtDNA), mitochondrial function, and autophagy in colorectal cell lines (HT-29)	0.5 mM/L	Reduced the number of mtDNA copies (indicative of a reduction in the number of mitochondria in these tumor cells).	Mitochondrial dysfunction	[306]

3. Metal Nanoparticles Elimination from Body

The elimination of NPs depends on their particle size, intrinsic biodegradability, core density, surface charge, and surface chemistry [307]. The liver is the major clearance organ in the oral administration of NPs. Intravenously administered NPs are cleared from the bloodstream by two main mechanisms: (i) renal elimination and (ii) hepatobiliary elimination. Choi et al. [308] reported that smaller-sized (<5.5 nm diameter) quantum dots undergo efficient urinary excretion due to the pore size limit of glomerular filtration in the kidneys. According to estimates of Si-NPs in rats, 7–8% of NPs were eliminated in urine and 75–80% were expelled in feces [309]. Nonbiodegradable and larger-sized (>5.5 nm) NPs are supposed to be eliminated through the hepatobiliary route. The hepatobiliary elimination involved the following pathways: (1) the liver sinusoid; (2) the space of Disse, a tiny perisinusoidal space containing blood plasma, nutrients, oxygen, and body waste that has become crucial in the treatment of liver disease, which is located between endothelial cells and hepatocytes; (3) hepatocytes; (4) bile ducts; (5) intestines; and finally (6) out of the body, as shown in Figure 11. In hepatobiliary elimination, the liver nonparenchymal cells (e.g., Kupffer cells and liver sinusoidal endothelial cells) influence and determine the elimination fate. The removal of Kupffer cells increased the fecal elimination of NPs by more than 10-fold [310].

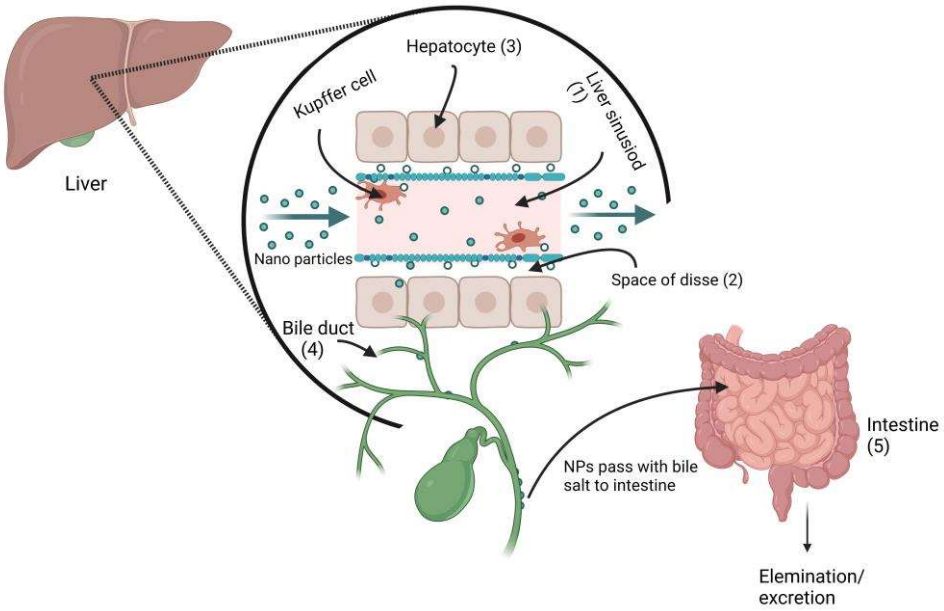

Figure 11. Proposed metal nanoparticles hepatobiliary clearance pathway (when metal NPs pass through the liver sinusoid, they enter the space of Disse via Kupffer cells, and then enter the bile duct, followed by fecal elimination.

NPs can enter the body through multiple routes, including the skin, respiratory tract, dermal exposure, mucosal, oral, intravenous, subcutaneous, intramuscular, etc., and can induce acute or chronic toxicities [311]. The anionic NPs are less toxic than the cationic NPs, which cause hemolysis and clotting [312]. Singh et al. [313] reported that ceramic NPs, commonly used for drug delivery, exhibit oxidative stress and cytotoxic activity in the lungs, liver, heart, and brain, as well as having teratogenic or carcinogenic effects. NPs have been shown, both in vivo and in vitro, to increase cellular reactive oxygen species, induce multiple minor and severe toxicities, and even disrupt host homeostasis [311]. Although NPs are useful for numerous medical applications, there are still some concerns for ecosystems and living organisms due to their uncontrollable use and discharge to the natural environment; thus, it should be considered to make the use of NPs more convenient and environmentally friendly. Preclinical studies have revealed the importance of renal-clearable luminous metal NPs in cancer therapy, which offers tremendous promise for

potential clinical translation [314]. The retention of NPs in the body, especially in the vital organs, usually depends on the density of the particles. In a study of gold and silver NPs by Tang et al., it was demonstrated that the lower-density metal NPs have a higher distribution and shorter retention time than the higher-density metal NPs [315].

4. Conclusions

Nanodrugs can be highlighted as the future of medicine, and using potential metals such as Fe, Au, Cu, Ag, Ni, and Zn in NPs showed optimistic results against various types of cancers, as well as displaying antitumor, antidiabetic, and antimicrobial activity. They are also applicable for other purposes, and it was found that metal NPs have significant synergistic activity with commercially available antibiotics. Since we already have certain levels of most metals in our bodies, they are compatible with our immune systems, which is of benefit to metal nanotherapy. Research has found that metals enhance the pharmacological activity considerably.

Despite recent advances in metal nanotherapy, the majority of nanotherapeutics are still being studied. The main concerns are not only their long-term safety for the patient, but also the ecological and toxicological aspects that need to be considered.

The generation of ROS is a significant challenge for metal NPs and metal oxide NPs. Diameter, structure, interface, content, solubility, accumulation, and particle absorption are factors that can affect ROS generation. A metallic nanomaterial's toxicity may vary based on its oxidation reaction, ligand, solubility, shape, environment, and medical factors. For example, characterization and cell type are important factors in the uptake of Au-NPs. If the Au-NPs are absorbed by a healthy cell, they will eventually be removed, but if they are absorbed by a malignant cell, they will cause cell death. More in vivo metal nanotherapeutic studies are needed to find out the toxicological conditions in normal cell lines when targeting cancer cells.

Author Contributions: T.I.: Conceptualization; M.M.R.: Methodology, M.N.M.: Methodology, I.A.: Methodology, M.T.I. (Md. Tariqul Islam): Resources, T.A.R.: Resources, A.C.J.A.: Software, J.M.F.d.L.S.: Software, B.C.G.V.d.L.: First draft of the manuscript, E.M.d.A.: First draft of the manuscript, M.A.K.: Resources, H.D.M.C.: Project administration, Z.H.: Supervision, M.T.I. (Muhammad Torequl Islam): Conceptualization; Supervision. All authors have read and agreed to the published version of the manuscript.

Funding: This research received no external funding.

Institutional Review Board Statement: Not applicable.

Informed Consent Statement: Not applicable.

Data Availability Statement: MDPI Research Data Policies.

Conflicts of Interest: The authors declare no conflict of interest.

References

1. Chandrasekhar, S.; Iyer, L.K.; Panchal, J.P.; Topp, E.M.; Cannon, J.B.; Ranade, V.V. Microarrays and microneedle arrays for delivery of peptides, proteins, vaccines and other applications. *Expert Opin. Drug Deliv.* **2013**, *10*, 1155–1170. [CrossRef]
2. Rabl, P.; Kolkowitz, S.J.; Koppens, F.H.L.; Harris, J.G.E.; Zoller, P.; Lukin, M.D. A quantum spin transducer based on nanoelectromechanical resonator arrays. *Nat. Phys.* **2010**, *6*, 602–608. [CrossRef]
3. Shabnashmi, P.S.; Naga Kani, S.; Vithya, V.; Vijaya Lakshmi, B.; Jasmine, R. Therapeutic applications of nanorobots-respirocytes and microbivores. *J. Chem. Pharm. Res.* **2016**, *8*, 605–609.
4. Kadam, R.S.; Bourne, D.W.; Kompella, U.B. Nano-advantage in enhanced drug delivery with biodegradable nanoparticles: Contribution of reduced clearance. *Drug Metab. Dispos.* **2012**, *40*, 1380–1388. [CrossRef] [PubMed]
5. Jahan, S.T.; Sadat, S.; Walliser, M.; Haddadi, A. Targeted therapeutic nanoparticles: An immense promise to fight against cancer. *J. Drug Deliv.* **2017**, *2017*, 1–24. [CrossRef] [PubMed]
6. Zhou, Y.; Peng, Z.; Seven, E.S.; Leblanc, R.M. Crossing the blood-brain barrier with nanoparticles. *J. Control. Release* **2018**, *270*, 290–303. [CrossRef] [PubMed]
7. Teleanu, D.M.; Chircov, C.; Grumezescu, A.M.; Volceanov, A.; Teleanu, R.I. Impact of nanoparticles on brain health: An up to date overview. *J. Clin. Med.* **2018**, *7*, 490. [CrossRef]

8. Rizvi, S.A.; Saleh, A.M. Applications of nanoparticle systems in drug delivery technology. *Saudi Pharm. J.* **2018**, *26*, 64–70. [CrossRef]
9. Thakkar, K.N.; Mhatre, S.S.; Parikh, R.Y. Biological synthesis of metallic nanoparticles. *Nanomed. Nanotechnol. Biol. Med.* **2010**, *6*, 257–262. [CrossRef]
10. Firdhouse, M.J.; Lalitha, P. Biosynthesis of silver nanoparticles and its applications. *J. Nanotechnol.* **2015**, *2015*, 18. [CrossRef]
11. Faraday, M.X. The Bakerian Lecture.—Experimental relations of gold (and other metals) to light. *Philos. Trans. R. Soc. Lond.* **1857**, *147*, 145–181.
12. Carver, P.L. Metals in medicine: The therapeutic use of metal ions in the clinic. *Essent. Met. Med. Ther. Use Toxic. Met. Ions Clin.* **2019**, *19*, 1–16.
13. Andreini, C.; Banci, L.; Bertini, I.; Rosato, A. Zinc through the three domains of life. *J. Proteome Res.* **2006**, *5*, 3173–3178. [CrossRef]
14. Maret, W. Metalloproteomics, metalloproteomes, and the annotation of metalloproteins. *Metallo* **2010**, *2*, 117–125. [CrossRef] [PubMed]
15. *Recommended Dietary Allowances*; National Research Council—National Academy Press: Washington, DC, USA, 1989.
16. Sigel, A.; Sigel, H.; Sigel, R.K. (Eds.) *Interrelations between Essential Metal Ions and Human Diseases*; Springer: Berlin/Heidelberg, Germany, 2013; Volume 13, pp. 81–137.
17. Ross, A.C.; Caballero, B.; Cousins, R.J.; Tucker, K.L. *Modern Nutrition in Health and Disease*; Jones & Bartlett Lear: Burlington, MA, USA, 2020.
18. Erdman, J.W., Jr.; Macdonald, I.A.; Zeisel, S.H. (Eds.) *Present Knowledge in Nutrition*; John and Wiley and Sons: Hoboken, NJ, USA, 2012.
19. Coates, P.M.; Paul, M.C.; Blackman, M.; Blackman, M.R.; Cragg, G.M.; Levine, M.; White, J.D.; Moss, J. (Eds.) *Encyclopedia of Dietary Supplements (Online)*; CRC Press: Boca Raton, FL, USA, 2004.
20. Abbaspour, N.; Hurrell, R.; Kelishadi, R. Review on iron and its importance for human health. *J. Res. Med. Sci.* **2014**, *19*, 164.
21. World Health Organization. *Worldwide Prevalence of Anaemia 1993–2005*; World Health Organization: Geneva, Switzerland, 2008.
22. Czarnek, K.; Terpiłowska, S.; Siwicki, A.K. Selected aspects of the action of cobalt ions in the human body. *Cent. Eur. J. Immunol.* **2015**, *40*, 236–242. [CrossRef]
23. Zdrojewicz, Z.; Popowicz, E.; Winiarski, J. Nickel-role in human organism and toxic effects. *Pol. Merkur. Lek. Organ Pol. Tow. Lek.* **2016**, *41*, 115–118.
24. Genchi, G.; Carocci, A.; Lauria, G.; Sinicropi, M.S.; Catalano, A. Nickel: Human health and environmental toxicology. *Int. J. Environ. Res. Public Health* **2020**, *17*, 679. [CrossRef]
25. Evens, R.; De Schamphelaere, K.A.; Janssen, C.R. The effects of dietary nickel exposure on growth and reproduction of Daphnia magna. *Aquat. Toxicol.* **2009**, *94*, 138–144. [CrossRef]
26. Kucharski, J.; Boros, E.; Wyszkowska, J. Biochemical Activity of Nickel-Contaminated Soil. *Pol. J. Environ. Stud.* **2009**, *18*, 1039–1044.
27. Hellman, N.E.; Gitlin, J.D. Ceruloplasmin metabolism and function. *Annu. Rev. Nutr.* **2002**, *22*, 439. [CrossRef] [PubMed]
28. Allen, K.G.; Klevay, L.M. Copper: An antioxidant nutrient for cardiovascular health. *Curr. Opin. Lipidol.* **1994**, *5*, 22–28. [CrossRef] [PubMed]
29. Sandstead, H.H. Understanding zinc: Recent observations and interpretations. *J. Lab. Clin. Med.* **1994**, *124*, 322–327. [PubMed]
30. Russell, R.; Beard, J.L.; Cousins, R.J.; Dunn, J.T.; Ferland, G.; Hambidge, K.; Lynch, S.; Penland, J.G.; Ross, A.C.; Stoecker, B.J.; et al. Dietary reference intakes for vitamin A, vitamin K, arsenic, boron, chromium, copper, iodine, iron, manganese, molybdenum, nickel, silicon, vanadium, and zinc. *Ins. Med.* **2001**, *2001*, 797.
31. Prasad, A.S. Zinc: An overview. *Nutrition* **1995**, *11*, 93–99. [PubMed]
32. Solomons, N.W. Mild human zinc deficiency produces an imbalance between cell-mediated and humoral immunity. *Nutr. Rev.* **1998**, *56*, 27–28. [CrossRef]
33. Heyneman, C.A. Zinc deficiency and taste disorders. *Ann. Pharmacoth.* **1996**, *30*, 186–187. [CrossRef]
34. Simmer, K.; Thompson, R.P.H. Zinc in the fetus and newborn. *Acta Paediatr.* **1985**, *74*, 158–163. [CrossRef]
35. Fabris, N.; Mocchegiani, E. Zinc, human diseases and aging. *Aging Clin. Exp. Res.* **1995**, *7*, 77–93. [CrossRef]
36. Maret, W.; Sandstead, H.H. Zinc requirements and the risks and benefits of zinc supplementation. *J. Trace Elements Med. Biol.* **2006**, *20*, 3–18. [CrossRef]
37. Prasad, A.S.; Beck, F.W.; Grabowski, S.M.; Kaplan, J.; Mathog, R.H. Zinc deficiency: Changes in cytokine production and T-cell subpopulations in patients with head and neck cancer and in noncancer subjects. *Proc. Assoc. Am.* **1997**, *109*, 68–77.
38. Rink, L. Zinc and the immune system. *Proc. Nutr. Soc.* **2000**, *59*, 541–552. [CrossRef] [PubMed]
39. Sravani, K.; Ketan, H.; Sanjay, S. A Review on Traditional Ayurvedic Preparations Containing Gold. *Int. J. Pharmacogn. Phytochem. Res.* **2017**, *9*, 801–807. [CrossRef]
40. Bagheri, S.; Yasemi, M.; Safaie-Qamsari, E.; Rashidiani, J.; Abkar, M.; Hassani, M.; Mirhosseini, S.A.; Kooshki, H. Using gold nanoparticles in diagnosis and treatment of melanoma cancer. *Nanomed. Biotech.* **2018**, *46*, 462–471. [CrossRef]
41. Hadjebi, M. Investigation on Triple Helical Cylinders' Effects on Human Osteosarcoma U2OS Cells. Ph.D. Thesis, University of Birmingham, Birmingham, UK, 2017.
42. Lopez, A.; Cacoub, P.; Macdougall, I.C.; Peyrin-Biroulet, L. Iron deficiency anaemia. *Lancet* **2016**, *387*, 907–916. [CrossRef]
43. Harth, M. Gold and modulation of the immune response. *J. Rheumatol.* **1979**, *5*, 7–11.

44. Ankamwar, B. Size and shape effect on biomedical applications of nanomaterials. In *Biomedical Engineering Technical Application in Medicine*; InTech: Rijeka, Croatia, 2012; pp. 93–114.
45. Albanese, A.; Tang, P.S.; Chan, W.C. The effect of nanoparticle size, shape, and surface chemistry on biological systems. *Annu. Rev. Biomed. Eng.* **2012**, *14*, 1–16. [CrossRef]
46. Sercombe, L.; Veerati, T.; Moheimani, F.; Wu, S.Y.; Sood, A.K.; Hua, S. Advances and challenges of liposome assisted drug delivery. *Front. Pharmacol.* **2015**, *6*, 286. [CrossRef]
47. Ahmad, Z.; Shah, A.; Siddiq, M.; Kraatz, H.B. Polymeric micelles as drug delivery vehicles. *RSC Adv.* **2014**, *4*, 17028–17038. [CrossRef]
48. Palmerston Mendes, L.; Pan, J.; Torchilin, V.P. Dendrimers as nanocarriers for nucleic acid and drug delivery in cancer therapy. *Molecules* **2017**, *22*, 1401. [CrossRef]
49. Kapusetti, G.; Misra, N.; Singh, V.; Srivastava, S.; Roy, P.; Dana, K.; Maiti, P. Bone cement based nanohybrid as a super biomaterial for bone healing. *J. Mater. Chem. B* **2014**, *2*, 3984–3997. [CrossRef]
50. Sharma, A.; Sharma, U.S. Liposomes in drug delivery: Progress and limitations. *Int. J. Pharm.* **1997**, *154*, 123–140. [CrossRef]
51. Soppimath, K.S.; Aminabhavi, T.M.; Kulkarni, A.R.; Rudzinski, W.E. Biodegradable polymeric nanoparticles as drug delivery devices. *J. Control. Release* **2001**, *70*, 1–20. [CrossRef] [PubMed]
52. Patel, S.; Kim, J.; Herrera, M.; Mukherjee, A.; Kabanov, A.V.; Sahay, G. Brief update on endocytosis of nanomedicines. *Adv. Drug Deliv. Rev.* **2019**, *144*, 90–111. [CrossRef]
53. Xu, S.; Olenyuk, B.Z.; Okamoto, C.T.; Hamm-Alvarez, S.F. Targeting receptor-mediated endocytotic pathways with nanoparticles: Rationale and advances. *Adv. Drug Deliv. Rev.* **2013**, *65*, 121–138. [CrossRef]
54. Sabourian, P.; Yazdani, G.; Ashraf, S.S.; Frounchi, M.; Mashayekhan, S.; Kiani, S.; Kakkar, A. Effect of physico-chemical properties of nanoparticles on their intracellular uptake. *Int. J. Mol. Sci.* **2020**, *21*, 8019. [CrossRef] [PubMed]
55. Janarthanan, G.; Noh, I. Recent trends in metal ion based hydrogel biomaterials for tissue engineering and other biomedical applications. *J. Mater. Sci. Technol.* **2021**, *63*, 35–53. [CrossRef]
56. Liu, N.; Zhu, S.; Deng, Y.; Xie, M.; Zhao, M.; Sun, T.; Yu, C.; Zhong, Y.; Guo, R.; Cheng, K.; et al. Construction of multifunctional hydrogel with metal-polyphenol capsules for infected full-thickness skin wound healing. *Bioact. Mater.* **2023**, *24*, 69–80. [CrossRef]
57. Pangli, H.; Vatanpour, S.; Hortamani, S.; Jalili, R.; Ghahary, A. Incorporation of silver nanoparticles in hydrogel matrices for controlling wound infection. *J. Burn. Care Res.* **2021**, *42*, 785–793. [CrossRef] [PubMed]
58. Zhao, C.; Liu, G.; Tan, Q.; Gao, M.; Chen, G.; Huang, X.; Xu, X.; Li, L.; Wang, J.; Zhang, Y.; et al. Polysaccharide-based biopolymer hydrogels for heavy metal detection and adsorption. *J. Adv. Res.* **2022**, *44*, 53–57. [CrossRef] [PubMed]
59. Bronstein, L.M.; Sidorov, S.N.; Valetsky, P.M.; Hartmann, J.; Cölfen, H.; Antonietti, M. Induced micellization by interaction of poly (2-vinylpyridine)-block-poly (ethylene oxide) with metal compounds. Micelle characteristics and metal nanoparticle formation. *Langmuir* **1999**, *15*, 6256–6262. [CrossRef]
60. Tan, H.L.; Teow, S.Y.; Pushpamalar, J. Application of metal nanoparticle–hydrogel composites in tissue regeneration. *Bioengineering* **2019**, *6*, 17. [CrossRef]
61. Gaucher, G.; Dufresne, M.H.; Sant, V.P.; Kang, N.; Maysinger, D.; Leroux, J.C. Block copolymer micelles: Preparation, characterization and application in drug delivery. *J. Control. Release* **2005**, *109*, 169–188. [CrossRef]
62. Rösler, A.; Vandermeulen, G.W.; Klok, H.A. Advanced drug delivery devices via self-assembly of amphiphilic block copolymers. *Adv. Drug Deliv. Rev.* **2012**, *64*, 270–279. [CrossRef]
63. Wu, M.L.; Chen, D.H.; Huang, T.C. Synthesis of Au/Pd bimetallic nanoparticles in reverse micelles. *Langmuir* **2001**, *17*, 3877–3883. [CrossRef]
64. Abbasi, E.; Aval, S.F.; Akbarzadeh, A.; Milani, M.; Nasrabadi, H.T.; Joo, S.W.; Hanifehpour, Y.; Nejati-Koshki, K.; Pashaei-Asl, R. Dendrimers: Synthesis, applications, and properties. *Nanoscale Res. Lett.* **2014**, *9*, 247. [CrossRef] [PubMed]
65. Rajca, A.; Utampanya, S. Dendrimer-based metal chelates: A new class of magnetic resonance imaging contrast agents. *J. Am. Chem. Soc.* **1993**, *115*, 10688. [CrossRef]
66. Crooks, R.M.; Zhao, M.; Sun, L.; Chechik, V.; Yeung, L.K. Dendrimer-encapsulated metal nanoparticles: Synthesis, characterization, and applications to catalysis. *Acc. Chem. Res.* **2001**, *34*, 181–190. [CrossRef]
67. Elsabahy, M.; Wooley, K.L. Design of polymeric nanoparticles for biomedical delivery applications. *Chem. Soc. Rev.* **2012**, *41*, 2545–2561. [CrossRef] [PubMed]
68. Kim, S.C.; Kim, D.W.; Shim, Y.H.; Bang, J.S.; Oh, H.S.; Kim, S.W.; Seo, M.H. In vivo evaluation of polymeric micellar paclitaxel formulation: Toxicity and efficacy. *J. Control. Release* **2001**, *72*, 191–202. [CrossRef]
69. Huh, K.M.; Kang, H.C.; Lee, Y.J.; Bae, Y.H. pH-sensitive polymers for drug delivery. *Macromol. Res.* **2012**, *20*, 224–233. [CrossRef]
70. Naz, M.; Nasiri, N.; Ikram, M.; Nafees, M.; Qureshi, M.Z.; Ali, S.; Tricoli, A. Eco-friendly biosynthesis, anticancer drug loading and cytotoxic effect of capped Ag-nanoparticles against breast cancer. *Appl. Nanosci.* **2017**, *7*, 793–802. [CrossRef]
71. Anselmo, A.C.; Mitragotri, S. A review of clinical translation of inorganic nanoparticles. *AAPS J.* **2015**, *17*, 1041–1054. [CrossRef]
72. Akbarzadeh, A.; Rezaei-Sadabady, R.; Davaran, S.; Joo, S.W.; Zarghami, N.; Hanifehpour, Y.; Samiei, M.; Kouhi, M.; Nejati-Koshki, K. Liposome: Classification, preparation, and applications. *Nanoscale Res. Lett.* **2013**, *8*, 102. [CrossRef]
73. Genç, R.; Clergeaud, G.; Ortiz, M.; O'sullivan, C.K. Green synthesis of gold nanoparticles using glycerol-incorporated nanosized liposomes. *Langmuir* **2011**, *27*, 10894–10900. [CrossRef] [PubMed]

74. Lee, J.H.; Shin, Y.; Lee, W.; Whang, K.; Kim, D.; Lee, L.P.; Choi, J.W.; Kang, T. General and programmable synthesis of hybrid liposome/metal nanoparticles. *Sci. Adv.* **2016**, *2*, e1601838. [CrossRef] [PubMed]
75. Paasonen, L.; Laaksonen, T.; Johans, C.; Yliperttula, M.; Kontturi, K.; Urtti, A. Gold nanoparticles enable selective light-induced contents release from liposomes. *J. Control. Release* **2007**, *122*, 86–93. [CrossRef] [PubMed]
76. Musielak, M.; Potoczny, J.; Boś-Liedke, A.; Kozak, M. The Combination of Liposomes and Metallic Nanoparticles as Multifunctional Nanostructures in the Therapy and Medical Imaging—A Review. *Int. J. Mol. Sci.* **2021**, *22*, 6229. [CrossRef]
77. Park, S.H.; Oh, S.G.; Suh, K.D.; Han, S.H.; Chung, D.J.; Mun, J.Y.; Han, S.S.; Kim, J.W. Control over micro-fluidity of liposomal membranes by hybridizing metal nanoparticles. *Colloids Surf. B Biointerfaces* **2009**, *70*, 108–113. [CrossRef]
78. Smith, I.O.; Liu, X.H.; Smith, L.A.; Ma, P.X. Nanostructured polymer scaffolds for tissue engineering and regenerative medicine. *Nanomed. Nanobiotechnol.* **2009**, *1*, 226–236. [CrossRef]
79. Biswas, A.; Amarajeewa, M.; Senapati, S.; Sahu, M.; Maiti, P. Sustained release of herbal drugs using biodegradable scaffold for faster wound healing and better patient compliance. *Nanomed. Nanotech. Biol. Med.* **2018**, *14*, 2131–2141. [CrossRef] [PubMed]
80. Abo-Shama, U.H.; El-Gendy, H.; Mousa, W.S.; Hamouda, R.A.; Yousuf, W.E.; Hetta, H.F.; Abdeen, E.E. Synergistic and antagonistic effects of metal nanoparticles in combination with antibiotics against some reference strains of pathogenic microorganisms. *Infect. Drug Resist.* **2020**, *2020*, 351–362. [CrossRef] [PubMed]
81. Kumari, S.; Singh, R.P. Glycolic acid-g-chitosan–Pt–Fe3O4 nanoparticles nanohybrid scaffold for tissue engineering and drug delivery. *Int. J. Biol. Macromol.* **2012**, *51*, 76–82. [CrossRef]
82. Arens, M.; Travis, S. Zinc salts inactivate clinical isolates of herpes simplex virus in vitro. *J. Clin. Microbiol.* **2000**, *38*, 1758–1762. [CrossRef] [PubMed]
83. Myint, Z.W.; Oo, T.H.; Thein, K.Z.; Tun, A.M.; Saeed, H. Copper deficiency anemia. *Ann. Hematol.* **2018**, *97*, 1527–1534. [CrossRef]
84. Sutton, B.M. Gold compounds for rheumatoid arthritis. *Gold Bull.* **1986**, *19*, 15–16. [CrossRef]
85. Fraser, T.N. Gold Treatment in Rheumatoid Arthritis. *Ann. Rheum. Dis.* **1945**, *4*, 71–75. [CrossRef] [PubMed]
86. Brewer, E.J., Jr.; Giannini, E.H.; Barkley, E. Gold therapy in the management of juvenile rheumatoid arthritis. *Arthritis Rheum.* **1980**, *23*, 404–411. [CrossRef]
87. Marguerie, L.; Flipo, R.-M.; Grardel, B.; Beaurain, D.; Duquesnoy, B.; Delcambre, B. Use of disease-modifying antirheumatic drugs in patients with psoriatic arthritis. *Jt. Bone Spine* **2002**, *69*, 275–281. [CrossRef]
88. Mattox, D.E.; Sternson, L.A.; Von Hoff, D.D.; Kuhn, J.G.; Repta, A. Tumor Concentration of Platinum in Patients with Head and Neck Cancer. *Otolaryngol. Neck Surg.* **1983**, *91*, 271–275. [CrossRef]
89. Prien, R.F.; Point, P.; Caffey, E.M.; Klett, C.J. Prophylactic efficacy of lithium carbonate in manic-depressive illness: Report of the Veterans Administration and National Institute of Mental Health Collaborative Study Group. *Arch. Gen. Psychiatry* **1973**, *28*, 337–341. [CrossRef]
90. Politano, A.D.; Campbell, K.T.; Rosenberger, L.H.; Sawyer, R.G. Use of Silver in the Prevention and Treatment of Infections: Silver Review. *Surg. Infect.* **2013**, *14*, 8–20. [CrossRef] [PubMed]
91. Yaqoob, A.A.; Ahmad, H.; Parveen, T.; Ahmad, A.; Oves, M.; Ismail, I.M.I.; Qari, H.A.; Umar, K.; Ibrahim, M.N.M. Recent Advances in Metal Decorated Nanomaterials and Their Various Biological Applications: A Review. *Front. Chem.* **2020**, *8*, 341. [CrossRef]
92. Kumar, H.; Venkatesh, N.; Bhowmik, H.; Kuila, A. Metallic nanoparticle: A review. *Biomed. J. Sci. Tech. Res.* **2018**, *4*, 3765–3775.
93. Fan, G.; Dundas, C.M.; Zhang, C.; Lynd, N.A.; Keitz, B.K. Sequence-dependent peptide surface functionalization of metal–organic frameworks. *ACS Appl. Mater. Interfaces* **2018**, *10*, 18601–18609. [CrossRef] [PubMed]
94. Joh, D.Y.; Sun, L.; Stangl, M.; Al Zaki, A.; Murty, S.; Santoiemma, P.P.; Davis, J.J.; Baumann, B.; Alonso-Basanta, M.; Bhang, D.; et al. Selective Targeting of Brain Tumors with Gold Nanoparticle-Induced Radiosensitization. *PLoS ONE* **2013**, *8*, e62425. [CrossRef]
95. Sun, W.; Karmakar, B.; Ibrahium, H.A.; Awwad, N.S.; El-Kott, A.F. Design and synthesis of nano Cu/chitosan-starch bio-composite for the treatment of human thyroid carcinoma. *Arab. J. Chem.* **2022**, *15*, 103465. [CrossRef]
96. Cho, S.H.; Jones, B.L.; Krishnan, S. The dosimetric feasibility of gold nanoparticle-aided radiation therapy (GNRT) via brachytherapy using low-energy gamma-/X-ray sources. *Phys. Med. Biol.* **2009**, *54*, 4889. [CrossRef]
97. Crosera, M.; Prodi, A.; Mauro, M.; Pelin, M.; Florio, C.; Bellomo, F.; Adami, G.; Apostoli, P.; De Palma, G.; Bovenzi, M.; et al. Titanium dioxide nanoparticle penetration into the skin and effects on HaCaT cells. *Int. J. Environ. Res. Public Health* **2015**, *12*, 9282–9297. [CrossRef] [PubMed]
98. Asharani, P.; Xinyi, N.; Hande, M.P.; Valiyaveettil, S. DNA damage and p53-mediated growth arrest in human cells treated with platinum nanoparticles. *Nanomedicine* **2010**, *5*, 51–64. [CrossRef] [PubMed]
99. Sabella, S.; Brunetti, V.; Vecchio, G.; Galeone, A.; Maiorano, G.; Cingolani, R.; Pompa, P.P. Toxicity of citrate-capped AuNPs: An in vitro and in vivo assessment. *J. Nanoparticle Res.* **2011**, *13*, 6821–6835. [CrossRef]
100. Shi, H.; Ye, X.; He, X.; Wang, K.; Cui, W.; He, D.; Li, D.; Jia, X. Au@ Ag/Au nanoparticles assembled with activatable aptamer probes as smart "nano-doctors" for image-guided cancer thermotherapy. *Nanoscale* **2014**, *6*, 8754–8761. [CrossRef]
101. Topete, A.; Alatorre-Meda, M.; Iglesias, P.; Villar-Alvarez, E.M.; Barbosa, S.; Costoya, J.A.; Taboada, P.; Mosquera, V. Fluorescent drug-loaded, polymeric-based, branched gold nanoshells for localized multimodal therapy and imaging of tumoral cells. *ACS Nano* **2014**, *8*, 2725–2738. [CrossRef] [PubMed]
102. Kumar, V.; Sharma, N.; Maitra, S.S. In vitro and in vivo toxicity assessment of nanoparticles. *Int. Nano Lett.* **2017**, *7*, 243–256. [CrossRef]

103. Bahadar, H.; Maqbool, F.; Niaz, K.; Abdollahi, M. Toxicity of Nanoparticles and an Overview of Current Experimental Models. *Iran. Biomed. J.* **2016**, *20*, 1.
104. Kim, D.-Y.; Kim, M.; Shinde, S.; Sung, J.-S.; Ghodake, G. Cytotoxicity and antibacterial assessment of gallic acid capped gold nanoparticles. *Colloids Surf. B Biointerfaces* **2017**, *149*, 162–167. [CrossRef]
105. Bhamidipati, M.; Fabris, L. Multiparametric assessment of gold nanoparticle cytotoxicity in cancerous and healthy cells: The role of size, shape, and surface chemistry. *Bioconjug. Chem.* **2017**, *28*, 449–460. [CrossRef] [PubMed]
106. Albanese, A.; Walkey, C.D.; Olsen, J.B.; Guo, H.; Emili, A.; Chan, W.C. Secreted biomolecules alter the biological identity and cellular interactions of nanoparticles. *ACS Nano* **2014**, *8*, 5515–5526. [CrossRef]
107. Girigoswami, K. Toxicity of metal oxide nanoparticles. Cellular and molecular toxicology of nanoparticles. *Adv. Exp. Med. Biol.* **2018**, *1048*, 99–122. [PubMed]
108. Bailly, A.L.; Correard, F.; Popov, A.; Tselikov, G.; Chaspoul, F.; Appay, R.; Al-Kattan, A.; Kabashin, A.V.; Braguer, D.; Esteve, M.A. In vivo evaluation of safety, biodistribution and pharmacokinetics of laser-synthesized gold nanoparticles. *Sci. Rep.* **2019**, *9*, 12890. [CrossRef]
109. Dai, Q.; Bertleff-Zieschang, N.; Braunger, J.A.; Björnmalm, M.; Cortez-Jugo, C.; Caruso, F. Particle targeting in complex biological media. *Adv. Healthc. Mater.* **2018**, *7*, 1700575. [CrossRef] [PubMed]
110. Daniel, M.C.; Astruc, D. Gold nanoparticles: Assembly, supramolecular chemistry, quantum-size-related properties, and applications toward biology, catalysis, and nanotechnology. *Chem. Rev.* **2004**, *104*, 293–346. [CrossRef] [PubMed]
111. Kodiha, M.; Wang, Y.M.; Hutter, E.; Maysinger, D.; Stochaj, U. Off to the organelles-killing cancer cells with targeted gold nanoparticles. *Theranostics* **2015**, *5*, 357. [CrossRef]
112. Basavegowda, N.; Idhayadhulla, A.; Lee, Y.R. Preparation of Au and Ag nanoparticles using Artemisia annua and their in vitro antibacterial and tyrosinase inhibitory activities. *Mater. Sci. Eng.* **2014**, *43*, 58–64. [CrossRef]
113. Bar, H.; Bhui, D.K.; Sahoo, G.P.; Sarkar, P.; Pyne, S.; Chattopadhyay, D.; Misra, A. Synthesis of gold nanoparticles of variable morphologies using aqueous leaf extracts of Cocculus hirsutus. *J. Exp. Nanosci.* **2012**, *7*, 109–119. [CrossRef]
114. Khan, A.U.; Yuan, Q.; Wei, Y.; Khan, G.M.; Khan, Z.U.H.; Khan, S.; Ali, F.; Tahir, K.; Ahmad, A.; Khan, F.U. Photocatalytic and antibacterial response of biosynthesized gold nanoparticles. *J. Photochem. Photobiol. B Biol.* **2016**, *162*, 273–277. [CrossRef] [PubMed]
115. Moradi, S.; Mokhtari-Dizaji, M.; Ghassemi, F.; Sheibani, S.; Amoli, F.A. The effect of ultrasound hyperthermia with gold nanoparticles on retinoblastoma Y79 cells. *Gold Bull.* **2020**, *53*, 111–120. [CrossRef]
116. Lu, W.; Singh, A.K.; Khan, S.A.; Senapati, D.; Yu, H.; Ray, P.C. Gold nano-popcorn-based targeted diagnosis, nanotherapy treatment, and in situ monitoring of photothermal therapy response of prostate cancer cells using surface-enhanced Raman spectroscopy. *J. Am. Chem. Soc.* **2010**, *132*, 18103–18114. [CrossRef]
117. Odion, R.; Liu, Y.; Vo-Dinh, T. Plasmonic gold nanostar-mediated photothermal immunotherapy. *IEEE J. Sel. Top. Quantum Electron.* **2021**, *27*, 4800109. [CrossRef] [PubMed]
118. Cheng, D.; Ji, Y.; Wang, B.; Wang, Y.; Tang, Y.; Fu, Y.; Xu, Y.; Qian, X.; Zhu, W. Dual-responsive nanohybrid based on degradable silica-coated gold nanorods for triple-combination therapy for breast cancer. *Acta Biomat.* **2021**, *128*, 435–446. [CrossRef] [PubMed]
119. Peng, C.; Xu, J.; Yu, M.; Ning, X.; Huang, Y.; Du, B.; Hernandez, E.; Kapur, P.; Hsieh, J.T.; Zheng, J. Tuning the in vivo transport of anticancer drugs using renal-clearable gold nanoparticles. *Angew. Chem.* **2019**, *131*, 8567–8571.
120. Kalimuthu, K.; Lubin, B.C.; Bazylevich, A.; Gellerman, G.; Shpilberg, O.; Luboshits, G.; Firer, M.A. Gold nanoparticles stabilize peptide-drug-conjugates for sustained targeted drug delivery to cancer cells. *J. Nanobiotechnol.* **2018**, *16*, 34. [CrossRef] [PubMed]
121. Farooq, M.U.; Novosad, V.; Rozhkova, E.A.; Wali, H.; Ali, A.; Fateh, A.A.; Neogi, P.B.; Neogi, A.; Wang, Z. Gold nanoparticles-enabled efficient dual delivery of anticancer therapeutics to HeLa cells. *Sci. Rep.* **2018**, *8*, 2907. [CrossRef] [PubMed]
122. Chithrani, B.D.; Ghazani, A.A.; Chan, W.C. Determining the size and shape dependence of gold nanoparticle uptake into mammalian cells. *Nano Lett.* **2006**, *6*, 662–668. [CrossRef]
123. Sze, J.H.; Raninga, P.V.; Nakamura, K.; Casey, M.; Khanna, K.K.; Berners-Price, S.J.; Di Trapani, G.; Tonissen, K.F. Anticancer activity of a Gold (I) phosphine thioredoxin reductase inhibitor in multiple myeloma. *Redox Biol.* **2020**, *28*, 101310. [CrossRef] [PubMed]
124. Patil, M.P.; Kim, G.D. Eco-friendly approach for nanoparticles synthesis and mechanism behind antibacterial activity of silver and anticancer activity of gold nanoparticles. *Appl. Microbiol. Biotechnol.* **2017**, *101*, 79–92. [CrossRef]
125. Baharara, J.; Ramezani, T.; Divsalar, A.; Mousavi, M.; Seyedarabi, A. Induction of apoptosis by green synthesized gold nanoparticles through activation of caspase-3 and 9 in human cervical cancer cells. *Avicenna J. Med. Biotechnol.* **2016**, *8*, 75.
126. Arshad, M.; Ozaslan, M.; Ali, H.K.; Safdar, M.; Junejo, Y.; Babar, M.E. Molecular Investigation of Gold Nanoparticles Toxicity in Mice Model and p53 Activation. *J. Biol. Sci.* **2019**, *19*, 391–395. [CrossRef]
127. Yu, M. and Zheng, J. Clearance pathways and tumor targeting of imaging nanoparticles. *ACS Nano* **2015**, *9*, 6655–6674. [CrossRef]
128. Sokary, R.; Abu el-naga, M.N.; Bekhit, M.; Atta, S. A potential antibiofilm, antimicrobial and anticancer activities of chitosan capped gold nanoparticles prepared by γ–irradiation. *Mater. Tech.* **2022**, *37*, 493–502. [CrossRef]
129. Yang, L.; Kim, T.H.; Cho, H.Y.; Luo, J.; Lee, J.M.; Chueng, S.T.D.; Hou, Y.; Yin, P.T.T.; Han, J.; Kim, J.H.; et al. Hybrid Graphene-Gold Nanoparticle-Based Nucleic Acid Conjugates for Cancer-Specific Multimodal Imaging and Combined Therapeutics. *Adv. Funct. Mater.* **2021**, *31*, 2006918. [CrossRef] [PubMed]

130. Akrami, M.; Samimi, S.; Alipour, M.; Bardania, H.; Ramezanpour, S.; Najafi, N.; Hosseinkhani, S.; Kamankesh, M.; Haririan, I.; Hassanshahi, F. Potential anticancer activity of a new pro-apoptotic peptide–thioctic acid gold nanoparticle platform. *Nanotechnology* **2021**, *32*, 145101. [CrossRef]
131. Xie, X.; Liao, J.; Shao, X.; Li, Q.; Lin, Y. The Effect of shape on Cellular Uptake of Gold Nanoparticles in the forms of Stars, Rods, and Triangles. *Sci. Rep.* **2017**, *7*, 3827. [CrossRef] [PubMed]
132. Scarabelli, L.; Coronado-Puchau, M.; Giner-Casares, J.J.; Langer, J.; Liz-Marzán, L.M. Monodisperse gold nanotriangles: Size control, large-scale self-assembly, and performance in surface-enhanced Raman scattering. *ACS Nano* **2014**, *8*, 5833–5842. [CrossRef] [PubMed]
133. Xiong, S.; Xiong, G.; Li, Z.; Jiang, Q.; Yin, J.; Yin, T.; Zheng, H. Gold nanoparticle-based nanoprobes with enhanced tumor targeting and photothermal/photodynamic response for therapy of osteosarcoma. *Nanotechnology* **2021**, *32*, 155102. [CrossRef]
134. Jana, B.; Kim, D.; Choi, H.; Kim, M.; Kim, K.; Kim, S.; Jin, S.; Park, M.-H.; Lee, K.H.; Yoon, C.; et al. Drug resistance-free cytotoxic nanodrugs in composites for cancer therapy. *J. Mater. Chem. B* **2021**, *9*, 3143–3152. [CrossRef]
135. Xu, Z.P.; Zeng, Q.H.; Lu, G.Q.; Yu, A.B. Inorganic nanoparticles as carriers for efficient cellular delivery. *Chem. Eng. Sci.* **2006**, *61*, 1027–1040. [CrossRef]
136. Vairavel, M.; Devaraj, E.; Shanmugam, R. An eco-friendly synthesis of Enterococcus sp.–mediated gold nanoparticle induces cytotoxicity in human colorectal cancer cells. *Environ. Sci. Pollut. Res.* **2020**, *27*, 8166–8175. [CrossRef]
137. Paciotti, G.F.; Zhao, J.; Cao, S.; Brodie, P.J.; Tamarkin, L.; Huhta, M.; Myer, L.D.; Friedman, J.; Kingston, D.G. Synthesis and evaluation of paclitaxel-loaded gold nanoparticles for tumor-targeted drug delivery. *Bioconjugate Chem.* **2016**, *27*, 2646–2657. [CrossRef]
138. Du, Y.; Xia, L.; Jo, A.; Davis, R.M.; Bissel, P.; Ehrich, M.F.; Kingston, D.G. Synthesis and evaluation of doxorubicin-loaded gold nanoparticles for tumor-targeted drug delivery. *Bioconjug. Chem.* **2018**, *29*, 420–430. [CrossRef] [PubMed]
139. Davidi, E.S.; Dreifuss, T.; Motiei, M.; Shai, E.; Bragilovski, D.; Lubimov, L.; Kindler, M.J.J.; Popovtzer, A.; Don, J.; Popovtzer, R. Cisplatin-conjugated gold nanoparticles as a theranostic agent for head and neck cancer. *Head Neck* **2018**, *40*, 70–78. [CrossRef]
140. Alamzadeh, Z.; Beik, J.; Mirrahimi, M.; Shakeri-Zadeh, A.; Ebrahimi, F.; Komeili, A.; Ghalandari, B.; Ghaznavi, H.; Kamrava, S.K.; Moustakis, C. Gold nanoparticles promote a multimodal synergistic cancer therapy strategy by co-delivery of thermo-chemo-radio therapy. *Eur. J. Pharm. Sci.* **2020**, *145*, 105235. [CrossRef]
141. Safwat, M.A.; Soliman, G.M.; Sayed, D.; Attia, M.A. Gold nanoparticles enhance 5-fluorouracil anticancer efficacy against colorectal cancer cells. *Int. J. Pharm.* **2016**, *513*, 648–658. [CrossRef]
142. Fathy, M.M.; Mohamed, F.S.; Elbialy, N.; Elshemey, W.M. Multifunctional Chitosan-Capped Gold Nanoparticles for enhanced cancer chemo-radiotherapy: An invitro study. *Phys. Med.* **2018**, *48*, 76–83. [CrossRef] [PubMed]
143. Yang, C.; Bromma, K.; Sung, W.; Schuemann, J.; Chithrani, D. Determining the radiation enhancement effects of gold nanoparticles in cells in a combined treatment with cisplatin and radiation at therapeutic megavoltage energies. *Cancers* **2018**, *10*, 150. [CrossRef]
144. Bannister, A.H.; Bromma, K.; Sung, W.; Monica, M.; Cicon, L.; Howard, P.; Chow, R.L.; Schuemann, J.; Chithrani, D.B. Modulation of nanoparticle uptake, intracellular distribution, and retention with docetaxel to enhance radiotherapy. *Br. J. Radiol.* **2020**, *92*, 20190742. [CrossRef]
145. Hussein, M.A.M.; Baños, F.G.D.; Grinholc, M.; Dena, A.S.A.; El-Sherbiny, I.M.; Megahed, M. Exploring the physicochemical and antimicrobial properties of gold-chitosan hybrid nanoparticles composed of varying chitosan amounts. *Int. J. Biol. Macromole* **2020**, *162*, 1760–1769. [CrossRef] [PubMed]
146. Vijayakumar, S.; Ganesan, S. Gold nanoparticles as an HIV entry inhibitor. *Curr. HIV Res.* **2012**, *10*, 643–646. [CrossRef]
147. Wani, I.A.; Ahmad, T. Size and shape dependant antifungal activity of gold nanoparticles: A case study of Candida. *Colloids Surf. B Biointer* **2013**, *101*, 162–170. [CrossRef] [PubMed]
148. Mocan, L.; Matea, C.; Tabaran, F.A.; Mosteanu, O.; Pop, T.; Puia, C.; Agoston-Coldea, L.; Gonciar, D.; Kalman, E.; Zaharie, G.; et al. Selective in vitro photothermal nano-therapy of MRSA infections mediated by IgG conjugated gold nanoparticles. *Sci. Rep.* **2016**, *6*, 39466. [CrossRef]
149. Omolaja, A.A.; Pearce, B.; Omoruyi, S.I.; Badmus, J.A.; Ismail, E.; Marnewick, J.; Botha, S.; Benjeddou, M.; Ekpo, O.E.; Hussein, A.A. The potential of chalcone-capped gold nanoparticles for the management of diabetes mellitus. *Surf. Interfaces* **2021**, *25*, 101251. [CrossRef]
150. Yogo, K.; Misawa, M.; Shimizu, M.; Shimizu, H.; Kitagawa, T.; Hirayama, R.; Ishiyama, H.; Furukawa, T.; Yasuda, H. Effect of gold nanoparticle radiosensitization on plasmid DNA damage induced by high-dose-rate brachytherapy. *Int. J. Nanomed.* **2021**, *16*, 359. [CrossRef]
151. Yuan, M.; Yan, T.H.; Li, J.; Xiao, Z.; Fang, Y.; Wang, Y.; Zhou, H.C.; Pellois, J.P. Superparamagnetic iron oxide–gold nanoparticles conjugated with porous coordination cages: Towards controlled drug release for non-invasive neuroregeneration. *Nanomed. Nanotechnol. Biol. Med.* **2021**, *35*, 102392. [CrossRef]
152. Liu, Y.; Chorniak, E.; Odion, R.; Etienne, W.; Nair, S.K.; Maccarini, P.; Palmer, G.M.; Inman, B.A.; Vo-Dinh, T. Plasmonic gold nanostars for synergistic photoimmunotherapy to treat cancer. *Nanophotonics* **2021**, *10*, 3295–3302. [CrossRef]
153. Sun, L.; Liu, Y.; Liu, X.; Wang, R.; Gong, J.; Saferali, A.; Gao, W.; Ma, A.; Ma, H.; Turvey, S.E.; et al. Nano-Enabled Reposition of Proton Pump Inhibitors for TLR Inhibition: Toward A New Targeted Nanotherapy for Acute Lung Injury. *Adv. Sci.* **2022**, *9*, 2104051. [CrossRef]

154. Jeremiah, S.S.; Miyakawa, K.; Morita, T.; Yamaoka, Y.; Ryo, A. Potent antiviral effect of silver nanoparticles on SARS-CoV-2. *Biochem. Biophys. Res. Commun.* **2020**, *533*, 195–200. [CrossRef] [PubMed]
155. Lara, H.H.; Ayala-Nuñez, N.V.; Ixtepan-Turrent, L.; Rodriguez-Padilla, C. Mode of antiviral action of silver nanoparticles against HIV-1. *J. Nanobiotechnol.* **2010**, *8*, 1–10. [CrossRef] [PubMed]
156. Rajan, A.; Vilas, V.; Philip, D. Studies on catalytic, antioxidant, antibacterial and anticancer activities of biogenic gold nanoparticles. *J. Mol. Liq.* **2015**, *212*, 331–339. [CrossRef]
157. Stępkowski, T.M.; Brzóska, K.; Kruszewski, M. Silver nanoparticles induced changes in the expression of NF-κB related genes are cell type specific and related to the basal activity of NF-κB. *Toxicol. In Vitro* **2014**, *28*, 473–478. [CrossRef]
158. Chang, X.; Wang, X.; Li, J.; Shang, M.; Niu, S.; Zhang, W.; Li, Y.; Sun, Z.; Gan, J.; Li, W.; et al. Silver nanoparticles induced cytotoxicity in HT22 cells through autophagy and apoptosis via PI3K/AKT/mTOR signaling pathway. *Ecotoxicol. Environ. Saf.* **2021**, *8*, 111696. [CrossRef]
159. Reddy, V.N.; Nyamathulla, S.; Pahirulzaman, K.A.K.; Mokhtar, S.I.; Giribabu, N.; Pasupuleti, V.R. Gallocatechin-silver nanoparticles embedded in cotton gauze patches accelerated wound healing in diabetic rats by promoting proliferation and inhibiting apoptosis through the Wnt/β-catenin signaling pathway. *PLoS ONE* **2022**, *17*, e0268505.
160. Spitzer, N.; Patterson, K.C.K.; Kipps, D.W. Akt and MAPK/ERK signaling regulate neurite extension in adult neural progenitor cells but do not directly mediate disruption of cytoskeletal structure and neurite dynamics by low-level silver nanoparticles. *Toxicol. In Vitro* **2021**, *74*, 105151. [CrossRef] [PubMed]
161. Parnsamut, C.; Brimson, S. Effects of silver nanoparticles and gold nanoparticles on IL-2, IL-6, and TNF-α production via MAPK pathway in leukemic cell lines. *Genet. Mol. Res.* **2015**, *14*, 3650–3668. [CrossRef] [PubMed]
162. Zhang, Y.; Hai, Y.; Miao, Y.; Qi, X.; Xue, W.; Luo, Y.; Fan, H.; Yue, T. The toxicity mechanism of different sized iron nanoparticles on human breast cancer (MCF7) cells. *Food Chem.* **2021**, *341*, 128263. [CrossRef] [PubMed]
163. Dobrucka, R.; Romaniuk-Drapała, A.; Kaczmarek, M. Facile synthesis of Au/ZnO/Ag nanoparticles using *Glechoma hederacea* L. extract, and their activity against leukemia. *Biomed. Microdevices* **2021**, *23*, 14. [CrossRef]
164. Al-Sheddi, E.S.; Farshori, N.N.; Al-Oqail, M.M.; Al-Massarani, S.M.; Saquib, Q.; Wahab, R.; Musarrat, J.; Al-Khedhairy, A.A.; Siddiqui, M.A. Anticancer potential of green synthesized silver nanoparticles using extract of *Nepeta deflersiana* against human cervical cancer cells (HeLA). *Bioinorg. Chem. Appl.* **2018**, *2018*, 9390784. [CrossRef]
165. Kuppusamy, P.; Ichwan, S.J.; Al-Zikri, P.N.H.; Suriyah, W.H.; Soundharrajan, I.; Govindan, N.; Maniam, G.P.; Yusoff, M.M. In vitro anticancer activity of Au, Ag nanoparticles synthesized using *Commelina nudiflora* L. aqueous extract against HCT-116 colon cancer cells. *Biol. Trace Elem. Res.* **2016**, *173*, 297–305. [CrossRef] [PubMed]
166. Yuan, Y.G.; Peng, Q.L.; Gurunathan, S. Silver nanoparticles enhance the apoptotic potential of gemcitabine in human ovarian cancer cells: Combination therapy for effective cancer treatment. *Int. J. Nanomed.* **2017**, *12*, 6487. [CrossRef] [PubMed]
167. Zielinska, E.; Zauszkiewicz-Pawlak, A.; Wojcik, M.; Inkielewicz-Stepniak, I. Silver nanoparticles of different sizes induce a mixed type of programmed cell death in human pancreatic ductal adenocarcinoma. *Oncotarget* **2018**, *9*, 4675. [CrossRef]
168. Nayak, D.; Ashe, S.; Rauta, P.R.; Kumari, M.; Nayak, B. Bark extract mediated green synthesis of silver nanoparticles: Evaluation of antimicrobial activity and antiproliferative response against osteosarcoma. *Mater. Sci. Eng. C* **2016**, *58*, 44–52. [CrossRef] [PubMed]
169. Lu, L.; Zhuang, Z.; Fan, M.; Liu, B.; Yang, Y.; Huang, J.; Da, X.; Mo, J.; Li, Q.; Lu, H. Green formulation of Ag nanoparticles by Hibiscus rosa-sinensis: Introducing a navel chemotherapeutic drug for the treatment of liver cancer. *Arab. J. Chem.* **2022**, *15*, 103602. [CrossRef]
170. Saber, M.M.; Mirtajani, S.B.; Karimzadeh, K. Green synthesis of silver nanoparticles using Trapa natans extract and their anticancer activity against A431 human skin cancer cells. *J. Drug Deliv. Sci. Technol.* **2018**, *47*, 375–379. [CrossRef]
171. Karekar, N.; Karan, A.; Khezerlou, E.; Prajapati, N.; Pernici, C.D.; Murray, T.A.; DeCoster, M.A. Self-Assembled metal–organic biohybrids (MOBs) using copper and silver for cell studies. *Nanomaterials* **2019**, *9*, 1282. [CrossRef]
172. Gahlawat, G.; Shikha, S.; Chaddha, B.S.; Chaudhuri, S.R.; Mayilraj, S.; Choudhury, A.R. Microbial glycolipoprotein-capped silver nanoparticles as emerging antibacterial agents against cholera. *Microb. Cell Factories* **2016**, *15*, 25. [CrossRef] [PubMed]
173. Praba, V.L.; Kathirvel, M.; Vallayyachari, K.; Surendar, K.; Muthuraj, M.; Jesuraj, P.J.; Govindarajan, S.; Raman, K.V. Bactericidal effect of silver nanoparticles against *Mycobacterium tuberculosis*. *J. Bionanosci.* **2013**, *7*, 282–287. [CrossRef]
174. Abdel-Aziz, M.M.; Yosri, M.; Amin, B.H. Control of imipenem resistant-*Klebsiella pneumoniae* pulmonary infection by oral treatment using a combination of mycosynthesized Ag-nanoparticles and imipenem. *J. Radiat. Res. Appl. Sci.* **2017**, *10*, 353–360. [CrossRef]
175. Mori, Y.; Ono, T.; Miyahira, Y.; Nguyen, V.Q.; Matsui, T.; Ishihara, M. Antiviral activity of silver nanoparticle/chitosan composites against H1N1 influenza A virus. *Nanoscale Res. Lett.* **2013**, *8*, 93. [CrossRef] [PubMed]
176. Dhanasezhian, A.; Srivani, S.; Govindaraju, K.; Parija, P.; Sasikala, S.; Kumar, M.R. Anti-Herpes Simplex Virus (HSV-1 and HSV-2) Activity of Biogenic Gold and Silver Nanoparticles Using Seaweed *Sargassum wightii*. *Indian J. Geo-Mar. Sci.* **2019**, *48*, 1252–1257.
177. Lu, L.; Sun, R.W.Y.; Chen, R.; Hui, C.K.; Ho, C.M.; Luk, J.M.; Lau, G.K.; Che, C.M. Silver nanoparticles inhibit hepatitis B virus replication. *Antivir. Ther.* **2008**, *13*, 253–262. [CrossRef] [PubMed]
178. Sharma, V.; Kaushik, S.; Pandit, P.; Dhull, D.; Yadav, J.P.; Kaushik, S. Green synthesis of silver nanoparticles from medicinal plants and evaluation of their antiviral potential against chikungunya virus. *Appl. Microbiol. Biotechnol.* **2019**, *103*, 881–891. [CrossRef]

179. Sujitha, V.; Murugan, K.; Paulpandi, M.; Panneerselvam, C.; Suresh, U.; Roni, M.; Nicoletti, M.; Higuchi, A.; Madhiyazhagan, P.; Subramaniam, J.; et al. Green-synthesized silver nanoparticles as a novel control tool against dengue virus (DEN-2) and its primary vector *Aedes aegypti*. *Parasitol. Res.* **2015**, *114*, 3315–3325. [CrossRef] [PubMed]
180. Sathishkumar, P.; Preethi, J.; Vijayan, R.; Yusoff, A.R.M.; Ameen, F.; Suresh, S.; Balagurunathan, R.; Palvannan, T. Anti-acne, anti-dandruff and anti-breast cancer efficacy of green synthesised silver nanoparticles using *Coriandrum sativum* leaf extract. *J. Photochem. Photobiol. B Biol.* **2016**, *163*, 69–76. [CrossRef]
181. Arceusz, A.; Wesolowski, M.; Konieczynski, P. NPC Natural Product Communications 2013. *NPC* **2013**, *8*, 1821. [PubMed]
182. Yang, Y.; Guo, L.; Wang, Z.; Liu, P.; Liu, X.; Ding, J.; Zhou, W. Targeted silver nanoparticles for rheumatoid arthritis therapy via macrophage apoptosis and Re-polarization. *Biomaterials* **2021**, *264*, 120390. [CrossRef] [PubMed]
183. Dong, Q.; Zu, D.; Kong, L.; Chen, S.; Yao, J.; Lin, J.; Lu, L.; Wu, B.; Fang, B. Construction of antibacterial nano-silver embedded bioactive hydrogel to repair infectious skin defects. *Biomater. Res.* **2022**, *26*, 36. [CrossRef]
184. Ibrahim, I.A.A.; Hussein, A.I.; Muter, M.S.; Mohammed, A.T.; Al-Medhtiy, M.H.; Shareef, S.H.; Aziz, P.Y.; Agha, N.F.S.; Abdulla, M.A. Effect of nano silver on gastroprotective activity against ethanol-induced stomach ulcer in rats. *Biomed. Pharmacother.* **2022**, *154*, 113550. [CrossRef]
185. Ponmurugan, P.; Manjukarunambika, K.; Elango, V.; Gnanamangai, B.M. Antifungal activity of biosynthesised copper nanoparticles evaluated against red root-rot disease in tea plants. *J. Exp. Nanosci.* **2016**, *11*, 1019–1031. [CrossRef]
186. Kiranmai, M.; Kadimcharla, K.; Keesara, N.R.; Fatima, S.N.; Bommena, P.; Batchu, U.R. Green synthesis of stable copper nanoparticles and synergistic activity with antibiotics. *Indian J. Pharm. Sci.* **2017**, *79*, 695–700.
187. Ghasemi, P.; Shafiee, G.; Ziamajidi, N.; Abbasalipourkabir, R. Copper Nanoparticles Induce Apoptosis and Oxidative Stress in SW480 Human Colon Cancer Cell Line. *Biol. Trace Elem. Res.* **2022**, *2022*, 1–9. [CrossRef]
188. Ghosh, S.; More, P.; Nitnavare, R.; Jagtap, S.; Chippalkatti, R.; Derle, A.; Kitture, R.; Asok, A.; Kale, S.; Singh, S.; et al. Antidiabetic and antioxidant properties of copper nanoparticles synthesized by medicinal plant *Dioscorea bulbifera*. *J. Nanomed. Nanotechnol.* **2015**, *S6*, 1.
189. Jung, S.; Yang, J.Y.; Byeon, E.Y.; Kim, D.G.; Lee, D.G.; Ryoo, S.; Lee, S.; Shin, C.W.; Jang, H.W.; Kim, H.J.; et al. Copper-coated polypropylene filter face mask with SARS-COV-2 antiviral ability. *Polymers* **2021**, *13*, 1367. [CrossRef]
190. Azizi, M.; Ghourchian, H.; Yazdian, F.; Dashtestani, F.; AlizadehZeinabad, H. Cytotoxic effect of albumin coated copper nanoparticle on human breast cancer cells of MDA-MB 231. *PLoS ONE* **2017**, *12*, e0188639. [CrossRef]
191. Lalitha, K.; Kalaimurgan, D.; Nithya, K.; Venkatesan, S.; Shivakumar, M.S. Antibacterial, antifungal and mosquitocidal efficacy of copper nanoparticles synthesized from entomopathogenic nematode: Insect–host relationship of bacteria in secondary metabolites of *Morganella morganii* sp. (PMA1). *Arabian J. Sci. Eng.* **2020**, *45*, 4489–4501. [CrossRef]
192. Sharon, E.A.; Velayutham, K.; Ramanibai, R. Biosynthesis of copper nanoparticles using *Artocarpus heterophyllus* against dengue vector *Aedes aegypti*. *Int. J. Life Sci. Sci. Res.* **2018**, *2455*, 1716. [CrossRef]
193. Hassanien, R.; Husein, D.Z.; Al-Hakkani, M.F. Biosynthesis of copper nanoparticles using aqueous Tilia extract: Antimicrobial and anticancer activities. *Heliyon* **2018**, *4*, e01077. [CrossRef] [PubMed]
194. Bramhanwade, K.; Shende, S.; Bonde, S.; Gade, A.; Rai, M. Fungicidal activity of Cu nanoparticles against Fusarium causing crop diseases. *Environ. Chem. Lett.* **2016**, *14*, 229–235. [CrossRef]
195. Hongfeng, Z.; El-Kott, A.; Ahmed, A.E.; Khames, A. Synthesis of chitosan-stabilized copper nanoparticles (CS-Cu NPs): Its catalytic activity for CN and CO cross-coupling reactions and treatment of bladder cancer. *Arab. J. Chem.* **2021**, *14*, 103259. [CrossRef]
196. Mukhopadhyay, R.; Kazi, J.; Debnath, M.C. Synthesis and characterization of copper nanoparticles stabilized with *Quisqualis indica* extract: Evaluation of its cytotoxicity and apoptosis in B16F10 melanoma cells. *Biomed. Pharmacother.* **2018**, *97*, 1373–1385. [CrossRef]
197. Valodkar, M.; Jadeja, R.N.; Thounaojam, M.C.; Devkar, R.V.; Thakore, S. Biocompatible synthesis of peptide capped copper nanoparticles and their biological effect on tumor cells. *Mater. Chem. Phys.* **2011**, *128*, 83–89. [CrossRef]
198. Chen, Q.; Huang, X.; Zhang, G.; Li, J.; Liu, Y.; Yan, X. Novel targeted pH-responsive drug delivery systems based on PEGMA-modified bimetallic Prussian blue analogs for breast cancer chemotherapy. *RSC Adv.* **2023**, *13*, 1684–1700. [CrossRef]
199. Harne, S.; Sharma, A.; Dhaygude, M.; Joglekar, S.; Kodam, K.; Hudlikar, M. Novel route for rapid biosynthesis of copper nanoparticles using aqueous extract of *Calotropis procera* L. latex and their cytotoxicity on tumor cells. *Colloids Surf. B Biointerfaces* **2012**, *95*, 284–288. [CrossRef] [PubMed]
200. Ai, J.W.; Liao, W.; Ren, Z.L. Enhanced anticancer effect of copper-loaded chitosan nanoparticles against osteosarcoma. *RSC Adv.* **2017**, *7*, 15971–15977. [CrossRef]
201. Prajapati, N.; Karan, A.; Khezerlou, E.; DeCoster, M.A. The immunomodulatory potential of copper and silver based self-assembled metal organic biohybrids nanomaterials in cancer theranostics. *Front. Chem.* **2021**, *8*, 629835. [CrossRef]
202. Sirotkin, A.V.; Radosová, M.; Tarko, A.; Martín-García, I.; Alonso, F. Effect of morphology and support of copper nanoparticles on basic ovarian granulosa cell functions. *Nanotoxicology* **2020**, *14*, 683–695. [CrossRef]
203. Albalawi, A.E.; Alanazi, A.D.; Alyousif, M.S.; Sepahvand, A.; Ebrahimi, K.; Niazi, M.; Mahmoudvand, H. The high potency of green synthesized copper nanoparticles to prevent the *Toxoplasma gondii* infection in mice. *Acta Parasitol.* **2021**, *66*, 1472–1479. [CrossRef] [PubMed]

204. Darder, M.; Karan, A.; Del Real, G.; DeCoster, M.A. Cellulose-based biomaterials integrated with copper-cystine hybrid structures as catalysts for nitric oxide generation. *Mater. Sci. Eng. C* **2020**, *108*, 110369. [CrossRef]
205. Jiménez-Holguín, J.; Sánchez-Salcedo, S.; Vallet-Regí, M.; Salinas, A.J. Development and evaluation of copper-containing mesoporous bioactive glasses for bone defects therapy. *Microporous Mesoporous Mater.* **2020**, *308*, 110454. [CrossRef]
206. Zhou, W.; Zi, L.; Cen, Y.; You, C.; Tian, M. Copper sulfide nanoparticles-incorporated hyaluronic acid injectable hydrogel with enhanced angiogenesis to promote wound healing. *Front. Bioeng. Biotechnol.* **2020**, *8*, 417. [CrossRef]
207. Ramesh, M.; Anbuvannan, M.; Viruthagiri, G. Green synthesis of ZnO nanoparticles using Solanum nigrum leaf extract and their antibacterial activity. *Acta Part A Mol. Biomol. Spectrosc.* **2015**, *136*, 864–870. [CrossRef]
208. Beyth, N.; Houri-Haddad, Y.; Domb, A.; Khan, W.; Hazan, R. Alternative antimicrobial approach: Nano-antimicrobial materials. *Evid.-Based Complement. Altern. Med.* **2015**, *2015*, 16. [CrossRef]
209. Wang, S.W.; Lee, C.H.; Lin, M.S.; Chi, C.W.; Chen, Y.J.; Wang, G.S.; Liao, K.W.; Chiu, L.P.; Wu, S.H.; Huang, D.M.; et al. ZnO nanoparticles induced caspase-dependent apoptosis in gingival squamous cell carcinoma through mitochondrial dysfunction and p70S6K signaling pathway. *Int. J. Mol. Sci.* **2020**, *21*, 1612. [CrossRef] [PubMed]
210. Gao, F.; Ma, N.; Zhou, H.; Wang, Q.; Zhang, H.; Wang, P.; Hou, H.; Wen, H.; Li, L. Zinc oxide nanoparticles-induced epigenetic change and G2/M arrest are associated with apoptosis in human epidermal keratinocytes. *Int. J. Nanomed.* **2016**, *11*, 3859.
211. Patrón-Romero, L.; Luque-Morales, P.A.; Loera-Castañeda, V.; Lares-Asseff, I.; Leal-Ávila, M.Á.; Alvelais-Palacios, J.A.; Plasencia-López, I.; Almanza-Reyes, H. Mitochondrial Dysfunction Induced by Zinc Oxide Nanoparticles. *Crystals* **2022**, *12*, 1089. [CrossRef]
212. Mishra, A.; Swain, R.K.; Mishra, S.K.; Panda, N.; Sethy, K. Growth performance and serum biochemical parameters as affected by nano zinc supplementation in layer chicks. *Indian J. Anim. Nutr.* **2014**, *31*, 384–388.
213. Selvakumari, D.; Deepa, R.; Mahalakshmi, V.; Subhashini, P.; Lakshminarayan, N. Anti cancer activity of ZnO nanoparticles on MCF7 (breast cancer cell) and A549 (lung cancer cell). *ARPN J. Eng. Appl. Sci.* **2015**, *10*, 5418–5421.
214. Kavithaa, K.; Paulpandi, M.; Ponraj, T.; Murugan, K.; Sumathi, S. Induction of intrinsic apoptotic pathway in human breast cancer (MCF-7) cells through facile biosynthesized zinc oxide nanorods. *Karbala Int. J. Mod. Sci.* **2016**, *2*, 46–55. [CrossRef]
215. Wu, R.; Wang, H.; Hai, L.; Wang, T.; Hou, M.; He, D.; He, X.; Wang, K. A photosensitizer-loaded zinc oxide-polydopamine core-shell nanotherapeutic agent for photodynamic and photothermal synergistic therapy of cancer cells. *Chin. Chem. Lett.* **2020**, *31*, 189–192. [CrossRef]
216. Malaikozhundan, B.; Vaseeharan, B.; Vijayakumar, S.; Pandiselvi, K.; Kalanjiam, M.A.R.; Murugan, K.; Benelli, G. Biological therapeutics of *Pongamia pinnata* coated zinc oxide nanoparticles against clinically important pathogenic bacteria, fungi and MCF-7 breast cancer cells. *Microb. Pathog.* **2017**, *104*, 268–277. [CrossRef] [PubMed]
217. Umar, H.; Kavaz, D.; Rizaner, N. Biosynthesis of zinc oxide nanoparticles using Albizia lebbeck stem bark, and evaluation of its antimicrobial, antioxidant, and cytotoxic activities on human breast cancer cell lines. *Int. J. Nanomed.* **2019**, *14*, 87. [CrossRef]
218. Kadhem, H.A.; Ibraheem, S.A.; Jabir, M.S.; Kadhim, A.A. Zainab Jihad taqi, and mihailescu dan florin, zinc oxide nanoparticles induce apoptosis in human breast cancer cells via caspase-8 and P53 pathway. *Nano Biomed. Eng.* **2019**, *11*, 35–43. [CrossRef]
219. Sadhukhan, P.; Kundu, M.; Chatterjee, S.; Ghosh, N.; Manna, P.; Das, J.; Sil, P.C. Targeted delivery of quercetin via pH-responsive zinc oxide nanoparticles for breast cancer therapy. *Mater. Sci. Eng. C* **2019**, *100*, 129–140. [CrossRef]
220. Shamasi, Z.; Es-haghi, A.; Taghavizadeh Yazdi, M.E.; Amiri, M.S.; Homayouni-Tabrizi, M. Role of Rubia tinctorum in the synthesis of zinc oxide nanoparticles and apoptosis induction in breast cancer cell line. *Nanomed. J.* **2021**, *8*, 65–72.
221. Sarala, E.; Madhukara Naik, M.; Vinuth, M.; Rami Reddy, Y.V.; Sujatha, H.R. Green synthesis of *Lawsonia inermis*-mediated zinc ferrite nanoparticles for magnetic studies and anticancer activity against breast cancer (MCF-7) cell lines. *J. Mater. Sci. Mater. Electron.* **2020**, *31*, 8589–8596. [CrossRef]
222. Aalami, A.H.; Mesgari, M.; Sahebkar, A. Synthesis and characterization of green zinc oxide nanoparticles with antiproliferative effects through apoptosis induction and microRNA modulation in breast cancer cells. *Bioinorg. Chem. Appl.* **2020**, *2020*, 17. [CrossRef]
223. Kc, B.; Paudel, S.N.; Rayamajhi, S.; Karna, D.; Adhikari, S.; Shrestha, B.G.; Bisht, G. Enhanced preferential cytotoxicity through surface modification: Synthesis, characterization and comparative in vitro evaluation of TritonX-100 modified and unmodified zinc oxide nanoparticles in human breast cancer cell (MDA-MB-231). *Chem. Cent. J.* **2016**, *10*, 16. [CrossRef] [PubMed]
224. Chakraborti, S.; Chakraborty, S.; Saha, S.; Manna, A.; Banerjee, S.; Adhikary, A.; Sarwar, S.; Hazra, T.K.; Das, T.; Chakrabarti, P. PEG-functionalized zinc oxide nanoparticles induce apoptosis in breast cancer cells through reactive oxygen species-dependent impairment of DNA damage repair enzyme NEIL2. *Free Radic. Biol. Med.* **2017**, *103*, 35–47. [CrossRef]
225. Ruenraroengsak, P.; Kiryushko, D.; Theodorou, I.G.; Klosowski, M.M.; Taylor, E.R.; Niriella, T.; Palmieri, C.; Yagüe, E.; Ryan, M.P.; Coombes, R.C.; et al. Frizzled-7-targeted delivery of zinc oxide nanoparticles to drug-resistant breast cancer cells. *Nanoscale* **2019**, *11*, 12858–12870. [CrossRef] [PubMed]
226. Shobha, N.; Nanda, N.; Giresha, A.S.; Manjappa, P.; Sophiya, P.; Dharmappa, K.K.; Nagabhushana, B.M. Synthesis and characterization of Zinc oxide nanoparticles utilizing seed source of *Ricinus communis* and study of its antioxidant, antifungal and anticancer activity. *Mater. Sci. Eng. C* **2019**, *97*, 842–850. [CrossRef] [PubMed]
227. Mahdizadeh, R.; Homayouni-Tabrizi, M.; Neamati, A.; Seyedi, S.M.R.; Tavakkol Afshari, H.S. Green synthesized-zinc oxide nanoparticles, the strong apoptosis inducer as an exclusive antitumor agent in murine breast tumor model and human breast cancer cell lines (MCF7). *J. Cell. Biochem.* **2019**, *120*, 17984–17993. [CrossRef]

228. Housseiny, M.; Gomaa, E. Enhancement of Antimicrobial and Antitumor Activities of Zinc Nanoparticles Biosynthesized by *Penicillium chrysogenum* AUMC 10608 Using Gamma Radiation. *Egypt. J. Bot.* **2019**, *59*, 319–337. [CrossRef]
229. Sharma, D.; Rajput, J.; Kaith, B.S.; Kaur, M.; Sharma, S. Synthesis of ZnO nanoparticles and study of their antibacterial and antifungal properties. *Thin Solid Films* **2010**, *519*, 1224–1229. [CrossRef]
230. Saravanan, M.; Gopinath, V.; Chaurasia, M.K.; Syed, A.; Ameen, F.; Purushothaman, N. Green synthesis of anisotropic zinc oxide nanoparticles with antibacterial and cytofriendly properties. *Microb. Pathog.* **2018**, *115*, 57–63. [CrossRef] [PubMed]
231. Praphakar, R.A.; Munusamy, M.A.; Alarfaj, A.A.; Kumar, S.S.; Rajan, M. Zn^{2+} cross-linked sodium alginate-g-allylamine-mannose polymeric carrier of rifampicin for macrophage targeting tuberculosis nanotherapy. *New J. Chem.* **2017**, *41*, 11324–11334. [CrossRef]
232. Hernández-Sierra, J.F.; Ruiz, F.; Pena, D.C.C.; Martínez-Gutiérrez, F.; Martínez, A.E.; Guillén, A.D.J.P.; Tapia-Pérez, H.; Castañón, G.M. The antimicrobial sensitivity of *Streptococcus mutans* to nanoparticles of silver, zinc oxide, and gold. *Nanomed. Nanotechnol. Biol. Med.* **2008**, *4*, 237–240. [CrossRef]
233. Raghupathi, K.R.; Koodali, R.T.; Manna, A.C. Size-dependent bacterial growth inhibition and mechanism of antibacterial activity of zinc oxide nanoparticles. *Langmuir* **2011**, *27*, 4020–4028. [CrossRef]
234. Kasi, G.; Viswanathan, K.; Sadeghi, K.; Seo, J. Optical, thermal, and structural properties of polyurethane in Mg-doped zinc oxide nanoparticles for antibacterial activity. *Prog. Org. Coat.* **2019**, *133*, 309–315. [CrossRef]
235. Banoee, M.; Seif, S.; Nazari, Z.E.; Jafari-Fesharaki, P.; Shahverdi, H.R.; Moballegh, A.; Moghaddam, K.M.; Shahverdi, A.R. ZnO nanoparticles enhanced antibacterial activity of ciprofloxacin against *Staphylococcus aureus* and *Escherichia coli*. *J. Biomed. Mater. Res. Part B Appl. Biomater.* **2010**, *93*, 557–561. [CrossRef]
236. Souza, J.M.T.; de Araujo, A.R.; de Carvalho, A.M.A.; Amorim, A.D.G.N.; Daboit, T.C.; de Almeida, J.R.D.S.; da Silva, D.A.; Eaton, P. Sustainably produced cashew gum-capped zinc oxide nanoparticles show antifungal activity against *Candida parapsilosis*. *J. Clean. Prod.* **2020**, *247*, 119085. [CrossRef]
237. Xie, Y.; He, Y.; Irwin, P.L.; Jin, T.; Shi, X. Antibacterial activity and mechanism of action of zinc oxide nanoparticles against *Campylobacter jejuni*. *Appl. Environ. Microbiol.* **2011**, *77*, 2325–2331. [CrossRef]
238. Dobrucka, R.; Długaszewska, J. Biosynthesis and antibacterial activity of ZnO nanoparticles using *Trifolium pratense* flower extract. *Saudi J. Biol. Sci.* **2016**, *23*, 517–523. [CrossRef]
239. Shaalan, M.I.; El-Mahdy, M.M.; Theiner, S.; El-Matbouli, M.; Saleh, M. In vitro assessment of the antimicrobial activity of silver and zinc oxide nanoparticles against fish pathogens. *Acta Vet. Scand.* **2017**, *59*, 49. [CrossRef] [PubMed]
240. Bhattacharyya, P.; Agarwal, B.; Goswami, M.; Maiti, D.; Baruah, S.; Tribedi, P. Zinc oxide nanoparticle inhibits the biofilm formation of *Streptococcus pneumoniae*. *Antonie Van Leeuwenhoe* **2018**, *111*, 89–99. [CrossRef] [PubMed]
241. He, S.; Guo, Z.; Zhang, Y.; Zhang, S.; Wang, J.; Gu, N. Biosynthesis of gold nanoparticles using the bacteria *Rhodopseudomonas capsulata*. *Mater. Lett.* **2007**, *61*, 3984–3987. [CrossRef]
242. Srinisha, M.; Rajeshkumar, S.; Lakshmi, T.; Roy, A. Amla fruit mediated synthesis of zinc oxide nanoparticles and its antifungal activity. *Int. J. Pharm. Sci.* **2019**, *10*, 2826–2829.
243. Sharma, R.K.; Ghose, R. Synthesis of zinc oxide nanoparticles by homogeneous precipitation method and its application in antifungal activity against *Candida albicans*. *Ceram. Int.* **2015**, *41*, 967–975. [CrossRef]
244. Jamdagni, P.; Rana, J.S.; Khatri, P.; Nehra, K. Comparative account of antifungal activity of green and chemically synthesized zinc oxide nanoparticles in combination with agricultural fungicides. *Int. J. Nano Dimens.* **2018**, *9*, 198–208.
245. Rajiv, P.; Rajeshwari, S.; Venckatesh, R. Bio-Fabrication of zinc oxide nanoparticles using leaf extract of *Parthenium hysterophorus* L. and its size-dependent antifungal activity against plant fungal pathogens. *Spectrochim. Acta Part A Mol. Biomol. Spectrosc.* **2013**, *112*, 384–387. [CrossRef]
246. El-Diasty, E.M.; Ahmed, M.A.; Okasha, N.A.G.W.A.; Mansour, S.F.; El-Dek, S.I.; El-Khalek, H.M.A.; Youssif, M.H. Antifungal activity of zinc oxide nanoparticles against dermatophytic lesions of cattle. *Rom. J. Biophys.* **2013**, *23*, 191–202.
247. Jasim, N.O. Antifungal activity of Zinc oxide nanoparticles on *Aspergillus fumigatus* fungus & *Candida albicans* yeast. *Citeseer* **2015**, *5*, 23–28.
248. Zhu, W.; Hu, C.; Ren, Y.; Lu, Y.; Song, Y.; Ji, Y.; Han, C.; He, J. Green synthesis of zinc oxide nanoparticles using *Cinnamomum camphora* (L.) Presl leaf extracts and its antifungal activity. *J. Environ. Chem. Eng.* **2021**, *9*, 106659. [CrossRef]
249. Al-Dhabaan, F.A.; Shoala, T.; Ali, A.A.; Alaa, M.; Abd-Elsalam, K.; Abd-Elsalam, K. Chemically-produced copper, zinc nanoparticles and chitosan-bimetallic nanocomposites and their antifungal activity against three phytopathogenic fungi. *Int. J. Agric. Technol.* **2017**, *13*, 753–769.
250. Umrani, R.D.; Paknikar, K.M. Zinc oxide nanoparticles show antidiabetic activity in streptozotocin-induced Type 1 and 2 diabetic rats. *Nanomedicine* **2014**, *9*, 89–104. [CrossRef] [PubMed]
251. Nazarizadeh, A.; Asri-Rezaie, S. Comparative study of antidiabetic activity and oxidative stress induced by zinc oxide nanoparticles and zinc sulfate in diabetic rats. *AAPS Pharm. Sci. Tech.* **2016**, *17*, 834–843. [CrossRef] [PubMed]
252. Govindan, N.; Vairaprakasam, K.; Chinnasamy, C.; Sivalingam, T.; Mohammed, M.K. Green synthesis of Zn-doped *Catharanthus roseus* nanoparticles for enhanced anti-diabetic activity. *Mater. Adv.* **2020**, *1*, 3460–3465. [CrossRef]
253. Siddiqui, S.A.; Or Rashid, M.; Uddin, M.; Robel, F.N.; Hossain, M.S.; Haque, M.; Jakaria, M. Biological efficacy of zinc oxide nanoparticles against diabetes: A preliminary study conducted in mice. *Biosci. Rep.* **2020**, *40*, 3972. [CrossRef]
254. Bayrami, A.; Parvinroo, S.; Habibi-Yangjeh, A.; Rahim Pouran, S. Bio-extract-mediated ZnO nanoparticles: Microwave-assisted synthesis, characterization and antidiabetic activity evaluation. *Artif. Cells Nanomed. Biotechnol.* **2018**, *46*, 730–739. [CrossRef]

255. Afifi, M.; Almaghrabi, O.A.; Kadasa, N.M. Ameliorative effect of zinc oxide nanoparticles on antioxidants and sperm characteristics in streptozotocin-induced diabetic rat testes. *BioMed Res. Int.* **2015**, *2015*, 153573. [CrossRef]
256. Ogunyemi, S.O.; Abdallah, Y.; Zhang, M.; Fouad, H.; Hong, X.; Ibrahim, E.; Masum, M.M.I.; Hossain, A.; Mo, J.; Li, B. Green synthesis of zinc oxide nanoparticles using different plant extracts and their antibacterial activity against *Xanthomonas oryzae* pv. oryzae. *Artif. Cells Nanomed. Biotechnol.* **2019**, *47*, 341–352. [CrossRef]
257. Abdel-Magied, N.; Shedid, S.M. Impact of zinc oxide nanoparticles on thioredoxin-interacting protein and asymmetric dimethylarginine as biochemical indicators of cardiovascular disorders in gamma-irradiated rats. *Environ. Toxicol.* **2020**, *35*, 430–442. [CrossRef]
258. El-Behery, E.I.; El-Naseery, N.I.; El-Ghazali, H.M.; Elewa, Y.H.; Mahdy, E.A.; El-Hady, E.; Konsowa, M.M. The efficacy of chronic zinc oxide nanoparticles using on testicular damage in the streptozotocin-induced diabetic rat model. *Acta Histochem.* **2019**, *121*, 84–93. [CrossRef]
259. Jeon, G.; Choi, H.; Park, D.J.; Nguyen, N.T.; Kim, Y.H.; Min, J. Melanin Treatment Effect of Vacuoles-Zinc Oxide Nanoparticles Combined with Ascorbic Acid. *Mol. Biotech.* **2022**, *2022*, 1–10. [CrossRef] [PubMed]
260. Adwin Jose, P.; Sankarganesh, M.; Dhaveethu Raja, J.; Senthilkumar, G.S.; Nandini Asha, R.; Raja, S.J.; Sheela, C.D. Bio-inspired nickel nanoparticles of pyrimidine-Schiff base: In vitro anticancer, BSA and DNA interactions, molecular docking and antioxidant studies. *J. Biomol. Struct. Dyn.* **2022**, *40*, 10715–10729. [CrossRef]
261. Jaji, N.D.; Lee, H.L.; Hussin, M.H.; Akil, H.M.; Zakaria, M.R.; Othman, M.B.H. Advanced nickel nanoparticles technology: From synthesis to applications. *Nanotechnol. Rev.* **2020**, *9*, 1456–1480. [CrossRef]
262. Rameshthangam, P.; Chitra, J.P. Synergistic anticancer effect of green synthesized nickel nanoparticles and quercetin extracted from *Ocimum sanctum* leaf extract. *J. Mater. Sci. Technol.* **2018**, *34*, 508–522. [CrossRef]
263. Gomaji Chaudhary, R.; Tanna, J.A.; Gandhare, N.V.; Rai, A.R.; Juneja, H.D. Synthesis of nickel nanoparticles: Microscopic investigation, an efficient catalyst and effective antibacterial activity. *Adv. Mater. Lett.* **2015**, *6*, 990–998. [CrossRef]
264. Ahghari, M.R.; Soltaninejad, V.; Maleki, A. Synthesis of nickel nanoparticles by a green and convenient method as a magnetic mirror with antibacterial activities. *Sci. Rep.* **2020**, *10*, 12627. [CrossRef] [PubMed]
265. Huang, Y.; Zhu, C.; Xie, R.; Ni, M. Green synthesis of nickel nanoparticles using Fumaria officinalis as a novel chemotherapeutic drug for the treatment of ovarian cancer. *J. Exp. Nanosci.* **2021**, *16*, 368–381. [CrossRef]
266. Magaye, R.R.; Yue, X.; Zou, B.; Shi, H.; Yu, H.; Liu, K.; Lin, X.; Xu, J.; Yang, C.; Wu, A.; et al. Acute toxicity of nickel nanoparticles in rats after intravenous injection. *Int. J. Nanomed.* **2014**, *9*, 1393.
267. Shwetha, U.R.; CR, R.K.; Kiran, M.S.; Betageri, V.S.; Latha, M.S.; Veerapur, R.; Lamraoui, G.; Al-Kheraif, A.A.; Elgorban, A.M.; Syed, A.; et al. Biogenic synthesis of NiO nanoparticles using areca catechu leaf extract and their antidiabetic and cytotoxic effects. *Molecules* **2021**, *26*, 2448.
268. Angajala, G.; Ramya, R.; Subashini, R. In-vitro anti-inflammatory and mosquito larvicidal efficacy of nickel nanoparticles phytofabricated from aqueous leaf extracts of *Aegle marmelos* Correa. *Acta Trop.* **2014**, *135*, 19–26. [CrossRef] [PubMed]
269. Rajakumar, G.; Rahuman, A.A.; Velayutham, K.; Ramyadevi, J.; Jeyasubramanian, K.; Marikani, A.; Elango, G.; Kamaraj, C.; Santhoshkumar, T.; Marimuthu, S.; et al. Novel and simple approach using synthesized nickel nanoparticles to control blood-sucking parasites. *Vet. Parasitol.* **2013**, *191*, 332–339. [CrossRef]
270. Jeyaraj Pandian, C.; Palanivel, R.; Dhanasekaran, S. Screening antimicrobial activity of nickel nanoparticles synthesized using *Ocimum sanctum* leaf extract. *J. Nanopart.* **2016**, *2016*, 4694367. [CrossRef]
271. Zarenezhad, E.; Abdulabbas, H.T.; Marzi, M.; Ghazy, E.; Ekrahi, M.; Pezeshki, B.; Ghasemian, A.; Moawad, A.A. Nickel Nanoparticles: Applications and Antimicrobial Role against Methicillin-Resistant *Staphylococcus aureus* Infections. *Antibiotics* **2022**, *11*, 1208. [CrossRef]
272. Wu, S.; Rajeshkumar, S.; Madasamy, M.; Mahendran, V. Green synthesis of copper nanoparticles using *Cissus vitiginea* and its antioxidant and antibacterial activity against urinary tract infection pathogens. *Artif. Cells Nanomed. Biotechnol.* **2020**, *48*, 1153–1158. [CrossRef] [PubMed]
273. Sudhasree, S.; Shakila Banu, A.; Brindha, P.; Kurian, G.A. Synthesis of nickel nanoparticles by chemical and green route and their comparison in respect to biological effect and toxicity. *Toxicol. Environ. Chem.* **2014**, *96*, 743–754. [CrossRef]
274. Shamaila, S.; Wali, H.; Sharif, R.; Nazir, J.; Zafar, N.; Rafique, M.S. Antibacterial effects of laser ablated Ni nanoparticles. *Appl. Phys. Lett.* **2013**, *103*, 153701. [CrossRef]
275. Haghshenas, L.; Faraji, A. Evaluation of the effect of Gold and Nickel nanoparticles on *Escherichia coli* and *Staphylococcus aurousbacteria* in milk. *J. Micro Nano Biomed.* **2016**, *1*, 1–6.
276. Vahedi, M.; Hosseini-Jazani, N.; Yousefi, S.; Ghahremani, M. Evaluation of anti-bacterial effects of nickel nanoparticles on biofilm production by *Staphylococcus epidermidis*. *Iran. J. Microbiol.* **2017**, *9*, 160.
277. Gorgizadeh, M.; Azarpira, N.; Lotfi, M.; Daneshvar, F.; Salehi, F.; Sattarahmady, N. Sonodynamic cancer therapy by a nickel ferrite/carbon nanocomposite on melanoma tumor: In vitro and in vivo studies. *Photodiagn. Photodyn. Ther.* **2019**, *27*, 27–33. [CrossRef]
278. Helan, V.; Prince, J.J.; Al-Dhabi, N.A.; Arasu, M.V.; Ayeshamariam, A.; Madhumitha, G.; Roopan, S.M.; Jayachandran, M. Neem leaves mediated preparation of NiO nanoparticles and its magnetization, coercivity and antibacterial analysis. *Results Phys.* **2016**, *6*, 712–718. [CrossRef]

279. Hoque, S.M.; Tariq, M.; Liba, S.I.; Salehin, F.; Mahmood, Z.H.; Khan, M.N.I.; Chattopadhayay, K.; Islam, R.; Akhter, S. Thermotherapeutic applications of chitosan-and PEG-coated $NiFe_2O_4$ nanoparticles. *Nanotechnology* **2016**, *27*, 285702. [CrossRef]
280. Huang, X.; Zhang, W.; Peng, Y.; Gao, L.; Wang, F.; Wang, L.; Wei, X. A multifunctional layered nickel silicate nanogenerator of synchronous oxygen self-supply and superoxide radical generation for hypoxic tumor therapy. *ACS Nano* **2021**, *16*, 974–983. [CrossRef]
281. Tombuloglu, H.; Albenayyan, N.; Slimani, Y.; Akhtar, S.; Tombuloglu, G.; Almessiere, M.; Baykal, A.; Ercan, I.; Sabit, H.; Manikandan, A. Fate and impact of maghemite (γ-Fe_2O_3) and magnetite (Fe_3O_4) nanoparticles in barley (*Hordeum vulgare* L.). *Environ. Sci. Pollut. Res.* **2022**, *29*, 4710–4721. [CrossRef] [PubMed]
282. Marand, Z.R.; Farimani, M.H.R.; Shahtahmasebi, N. Study of magnetic and structural and optical properties of Zn doped Fe_3O_4 nanoparticles synthesized by co-precipitation method for biomedical application. *Akush. Ginekol.* **2014**, *15*, 238–247.
283. Ding, W.; Guo, L. Immobilized transferrin Fe_3O_4@SiO_2 nanoparticle with high doxorubicin loading for dual-targeted tumor drug delivery. *Int. J. Nanomed.* **2013**, *8*, 4631–4639.
284. Zhang, H.; Li, T.; Luo, W.; Peng, G.X.; Xiong, J. Green synthesis of Ag nanoparticles from *Leucus aspera* and its application in anticancer activity against alveolar cancer. *J. Exp. Nanosci.* **2021**, *17*, 47–60. [CrossRef]
285. Arriortua, O.K.; Garaio, E.; de la Parte, B.H.; Insausti, M.; Lezama, L.; Plazaola, F.; García, J.A.; Aizpurua, J.M.; Sagartzazu, M.; Irazola, M.; et al. Antitumor magnetic hyperthermia induced by RGD-functionalized Fe_3O_4 nanoparticles, in an experimental model of colorectal liver metastases. *Beilstein J. Nanotech.* **2016**, *7*, 1532–1542. [CrossRef]
286. Kalber, T.L.; Ordidge, K.L.; Southern, P.; Loebinger, M.R.; Kyrtatos, P.G.; Pankhurst, Q.A.; Lythgoe, M.F.; Janes, S.M. Hyperthermia treatment of tumors by mesenchymal stem cell-delivered superparamagnetic iron oxide nanoparticles. *Int. J. Nanomed.* **2016**, *11*, 1973. [CrossRef]
287. Hedayatnasab, Z.; Dabbagh, A.; Abnisa, F.; Daud, W.M.A.W. Polycaprolactone-coated superparamagnetic iron oxide nanoparticles for in vitro magnetic hyperthermia therapy of cancer. *Eur. Poly. J.* **2020**, *133*, 109789. [CrossRef]
288. Hsieh, C.H.; Hsieh, H.C.; Shih, F.H.; Wang, P.W.; Yang, L.X.; Shieh, D.B.; Wang, Y.C. An innovative NRF2 nano-modulator induces lung cancer ferroptosis and elicits an immunostimulatory tumor microenvironment. *Theranostics* **2021**, *11*, 7072. [CrossRef]
289. Ismail, R.A.; Sulaiman, G.M.; Abdulrahman, S.A.; Marzoog, T.R. Antibacterial activity of magnetic iron oxide nanoparticles synthesized by laser ablation in liquid. *Mater. Sci. Eng.* **2015**, *53*, 286–297. [CrossRef] [PubMed]
290. Mahdy, S.A.; Raheed, Q.J.; Kalaichelvan, P.T. Antimicrobial activity of zero-valent iron nanoparticles. *Int. J. Mod. Eng. Res.* **2012**, *2*, 578–581.
291. Kumar, R.; Nayak, M.; Sahoo, G.C.; Pandey, K.; Sarkar, M.C.; Ansari, Y.; Das, V.N.R.; Topno, R.K.; Madhukar, M.; Das, P. Iron oxide nanoparticles based antiviral activity of H1N1 influenza A virus. *J. Infect. Chemother.* **2019**, *25*, 325–329. [CrossRef] [PubMed]
292. Parveen, S.; Wani, A.H.; Shah, M.A.; Devi, H.S.; Bhat, M.Y.; Koka, J.A. Preparation, characterization and antifungal activity of iron oxide nanoparticles. *Microb. Pathog.* **2018**, *115*, 287–292. [CrossRef]
293. Wang, Y.; Liu, T.; Li, X.; Sheng, H.; Ma, X.; Hao, L. Ferroptosis-inducing nanomedicine for cancer therapy. *Front. Pharm.* **2021**, *12*, 3638. [CrossRef]
294. Wen, J.; Chen, H.; Ren, Z.; Zhang, P.; Chen, J.; Jiang, S. Ultrasmall iron oxide nanoparticles induced ferroptosis via Beclin1/ATG5-dependent autophagy pathway. *Nano Converg.* **2021**, *8*, 10. [CrossRef]
295. Bhinge, S.; Bhutkar, M.; Randive, D.; Wadkar, G.; Todkar, S. Synergistic effects of synthesized iron nanoparticles of neem extract with conventional antibiotic against gram positive negative microorganism. *Int. J. Infect. Dis.* **2020**, *101*, 48. [CrossRef]
296. Padilla-Cruz, A.L.; Garza-Cervantes, J.A.; Vasto-Anzaldo, X.G.; García-Rivas, G.; León-Buitimea, A.; Morones-Ramírez, J.R. Synthesis and design of Ag–Fe bimetallic nanoparticles as antimicrobial synergistic combination therapies against clinically relevant pathogens. *Sci. Rep.* **2021**, *11*, 5351. [CrossRef]
297. Chen, Q.; Ma, X.; Xie, L.; Chen, W.; Xu, Z.; Song, E.; Zhu, X.; Song, Y. Iron-based nanoparticles for MR imaging-guided ferroptosis in combination with photodynamic therapy to enhance cancer treatment. *Nanoscale* **2021**, *13*, 4855–4870. [CrossRef]
298. Moghadam, S.M.M.; Alibolandi, M.; Babaei, M.; Mosafer, J.; Saljooghi, A.S.; Ramezani, M. Fabrication of deferasirox-decorated aptamer-targeted superparamagnetic iron oxide nanoparticles (SPION) as a therapeutic and magnetic resonance imaging agent in cancer therapy. *JBIC J. Biol. Inorg. Chem.* **2021**, *26*, 29–41. [CrossRef]
299. Farshchi, H.K.; Azizi, M.; Jaafari, M.R.; Nemati, S.H.; Fotovat, A. Green synthesis of iron nanoparticles by Rosemary extract and cytotoxicity effect evaluation on cancer cell lines. *Biocatal. Agric. Biotechnol.* **2018**, *16*, 54–62. [CrossRef]
300. Li, W.; Yu, H.; Ding, D.; Chen, Z.; Wang, Y.; Wang, S.; Li, X.; Keidar, M.; Zhang, W. Cold atmospheric plasma and iron oxide-based magnetic nanoparticles for synergetic lung cancer therapy. *Free Radic. Biol. Med.* **2019**, *130*, 71–81. [CrossRef] [PubMed]
301. Poller, J.M.; Zaloga, J.; Schreiber, E.; Unterweger, H.; Janko, C.; Radon, P.; Eberbeck, D.; Trahms, L.; Alexiou, C.; Friedrich, R.P. Selection of potential iron oxide nanoparticles for breast cancer treatment based on in vitro cytotoxicity and cellular uptake. *Int. J. Nanomed.* **2017**, *12*, 3207. [CrossRef] [PubMed]
302. Yu, C.; Ding, B.; Zhang, X.; Deng, X.; Deng, K.; Cheng, Z.; Xing, B.; Jin, D.; Lin, J. Targeted iron nanoparticles with platinum-(IV) prodrugs and anti-EZH2 siRNA show great synergy in combating drug resistance in vitro and in vivo. *Biomaterials* **2018**, *155*, 112–123. [CrossRef]
303. Hajsalimi, G.; Taheri, S.; Shahi, F.; Attar, F.; Ahmadi, H.; Falahati, M. Interaction of iron nanoparticles with nervous system: An in vitro study. *J. Biomol. Struct. Dyn.* **2018**, *36*, 928–937. [CrossRef] [PubMed]

304. Dheyab, M.A.; Aziz, A.A.; Jameel, M.S.; Khaniabadi, P.M.; Mehrdel, B.; Khaniabadi, B.M. Gold-coated iron oxide nanoparticles as a potential photothermal therapy agent to enhance eradication of breast cancer cells. *J. Phys. Conf. Ser.* **2020**, *1497*, 012003. [CrossRef]
305. Miri, A.; Najafzadeh, H.; Darroudi, M.; Miri, M.J.; Kouhbanani, M.A.J.; Sarani, M. Iron oxide nanoparticles: Biosynthesis, magnetic behavior, cytotoxic effect. *ChemistryOpen* **2021**, *10*, 327–333. [CrossRef]
306. Rivas-García, L.; Quiles, J.L.; Varela-López, A.; Giampieri, F.; Battino, M.; Bettmer, J.; Montes-Bayón, M.; Llopis, J.; Sánchez-González, C. Ultra-small iron nanoparticles target mitochondria inducing autophagy, acting on mitochondrial dna and reducing respiration. *Pharmaceutics* **2021**, *13*, 90. [CrossRef]
307. Du, B.; Yu, M.; Zheng, J. Transport and interactions of nanoparticles in the kidneys. *Nat. Rev. Mater.* **2018**, *3*, 358–374. [CrossRef]
308. Soo Choi, H.; Liu, W.; Misra, P.; Tanaka, E.; Zimmer, J.P.; Itty Ipe, B.; Bawendi, M.G.; Frangioni, J.V. Renal clearance of quantum dots. *Nat. Biotechnol.* **2007**, *25*, 1165–1170. [CrossRef]
309. Lee, J.A.; Kim, M.K.; Paek, H.J.; Kim, Y.R.; Kim, M.K.; Lee, J.K.; Jeong, J.; Choi, S.J. Tissue distribution and excretion kinetics of orally administered silica nanoparticles in rats. *Int. J. Nanomed.* **2014**, *9*, 251.
310. Poon, W.; Zhang, Y.N.; Ouyang, B.; Kingston, B.R.; Wu, J.L.; Wilhelm, S.; Chan, W.C. Elimination pathways of nanoparticles. *ACS Nano* **2019**, *13*, 5785–5798. [CrossRef]
311. Chenthamara, D.; Subramaniam, S.; Ramakrishnan, S.G.; Krishnaswamy, S.; Essa, M.M.; Lin, F.H.; Qoronfleh, M.W. Therapeutic efficacy of nanoparticles and routes of administration. *Biomater. Res.* **2019**, *23*, 20. [CrossRef]
312. De Jong, W.H.; Hagens, W.I.; Krystek, P.; Burger, M.C.; Sips, A.J.; Geertsma, R.E. Particle size-dependent organ distribution of gold nanoparticles after intravenous administration. *Biomaterials* **2008**, *29*, 1912–1919. [CrossRef] [PubMed]
313. Singh, D.; Singh, S.; Sahu, J.; Srivastava, S.; Singh, M.R. Ceramic nanoparticles: Recompense, cellular uptake and toxicity concerns. *Artif. Cells Nanomed. Biotechnol.* **2016**, *44*, 401–409. [CrossRef] [PubMed]
314. Liu, T.; Chao, Y.; Gao, M.; Liang, C.; Chen, Q.; Song, G.; Cheng, L.; Liu, Z. Ultra-small MoS2 nanodots with rapid body clearance for photothermal cancer therapy. *Nano Res.* **2016**, *9*, 3003–3017. [CrossRef]
315. Tang, S.; Peng, C.; Xu, J.; Du, B.; Wang, Q.; Vinluan, R.D., 3rd; Yu, M.; Kim, M.J.; Zheng, J. Tailoring renal clearance and tumor targeting of ultrasmall metal nanoparticles with particle density. *Angew. Chem. Int. Ed.* **2016**, *55*, 16039–16043. [CrossRef] [PubMed]